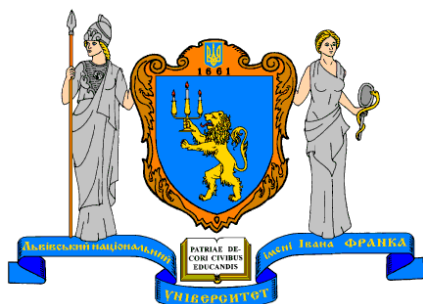
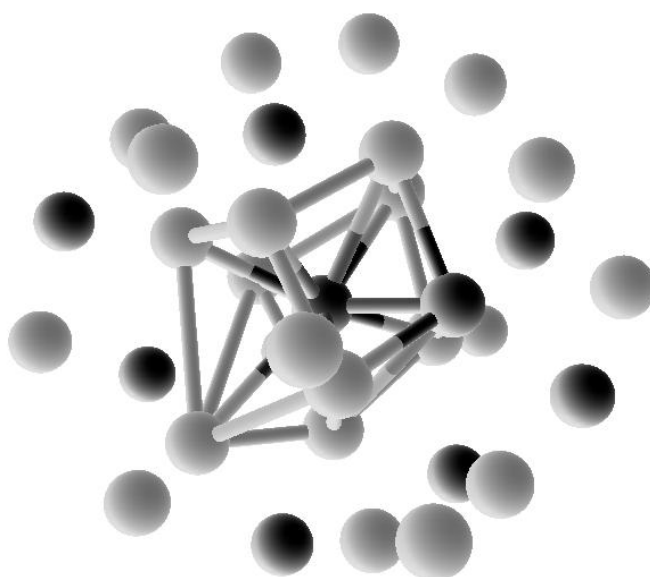


Міністерство освіти і науки України  
Львівський національний університет імені Івана Франка  
Фізичний факультет



**МАТЕРІАЛИ**  
**IX Міжнародної наукової конференції**  
**“Фізика неупорядкованих систем”,**



*19-20 вересня 2023р.*

**ЛЬВІВ, УКРАЇНА**

**Фізика неупорядкованих систем.** Збірник тез, Львів, Україна, 19-20 вересня 2023, Львівський національний університет імені Івана Франка, 79с.

На конференції заслухано доповіді за результатами наукових досліджень з найактуальніших досягнень у різних напрямках фізики неупорядкованих систем і нанокompозити на їх основі, включаючи: структуру, структурно-чутливі властивості, фазові переходи, поверхневі явища, критичні явища, магнетизм, електронні процеси.

Матеріали надруковано в авторській редакції

Фізичний факультет, кафедра фізики металів,  
вул. Кирила і Мефодія, 8, Львів, 79005, Україна  
**E-mail:** pds2023@lnu.edu.ua  
**Web:** <http://physics.lnu.edu.ua/pds2023/>

Львівський національний університет імені Івана Франка,  
Львів, 2023

## Секція 1

*Структура та фізичні властивості розплавів та  
молекулярних рідин.*

## The structure of ternary $\text{Al}_{80-x}\text{M}_{20}\text{Sn}_x$ (M=Fe, Co, Ni) melts

Roik O.S., Yakovenko O.M., Kazimirov V.P., Kashyrina Y.O., Sokolskii V.E.

*Taras Shevchenko National University of Kyiv, Ukraine*

The structure of the melts along the  $\text{Al}_{80-x}\text{M}_{20}\text{Sn}_x$  (M=Fe, Co, Ni) section was studied using the X-ray diffraction method in a purified helium atmosphere. The main goal of the present study was to assess the influence of the energetics of paired interatomic interactions on the formation of the SRO of the investigated ternary melts. The quantitative assessment of the energy factor was based on the mixing enthalpy ( $\Delta H_{\text{mix}}$ ) of the boundary binary melts, which is characterized by noticeable negative values and an increase in exothermicity in the row  $\text{Al-Fe} \rightarrow \text{Al-Co} \rightarrow \text{Al-Ni}$ , positive values of  $\Delta H_{\text{mix}}$  for Al-Sn, Fe-Sn melts and negative values of  $\Delta H_{\text{mix}}$  for Co-Sn, Ni-Sn melts.

Significant energy non-equivalence of heteroatomic interactions Al-Fe and Sn-Fe, Al-Co and Sn-Co, Al-Ni and Sn-Ni in boundary binary melts cause an effect of competition between Al and Sn atoms in the formation of the SRO around Fe, Co or Ni atoms in ternary melts. This competition, as well as a bigger radius of Sn atoms, results in the formation of atomic clusters with liquid Sn-like SRO that is manifested in the form of an influx on the low-angle side of the first peak of the structure factor  $S(Q)$  of ternary melts at  $\chi_{\text{Sn}} \geq 28$  at.%. The position of the influx coincides with the position of the first peak of  $S(Q)$  for liquid tin, which points out the micro-inhomogeneous structure. An increase in the tin content leads to the transformation of the influx into a separate peak, while  $S(Q)$  curves of ternary melt with  $\chi_{\text{Sn}} = 55$  at.% practically coincide with the structure factor of pure liquid tin. The concentration dependence of  $R_1$  for ternary melts is characterized by positive deviations from additivity at  $\chi_{\text{Sn}} > 28$  at.%, which increase noticeably in the row  $\text{Al}_{80-x}\text{Fe}_{20}\text{Sn}_x \rightarrow \text{Al}_{80-x}\text{Co}_{20}\text{Sn}_x \rightarrow \text{Al}_{80-x}\text{Ni}_{20}\text{Sn}_x$ .

Additionally, the SRO in the liquid  $\text{Al}_{80-x}\text{M}_{20}\text{Sn}_x$  (M=Fe, Co, Ni) alloys has been investigated using Reverse Monte Carlo simulations. The existence of two kinds of atomic clusters with different SRO reveals itself in the complex shape of the first peak on partial structure factor  $S_{\text{SnSn}}(Q)$ . The obtained results indicate two-structural states of Sn atoms in the investigated ternary melts: as part of clusters with the Sn-like local atomic structure and clusters with chemical short-range order.

# One-dimensionally confined water and ammonia molecules in single-wall carbon nanotubes

Krasnov V., Druchok M., Krokhmalski T., Derzhko O.

*Institute for Condensed Matter Physics, National Academy of Sciences of Ukraine, L'viv, Ukraine*

We examine a single-file chain of water and ammonia molecules in narrow single-wall carbon nanotubes (SWCNTs). To this end, we use molecular dynamics simulations (combined with the charges for water oxygen, ammonia nitrogen and hydrogen for both molecules obtained from quantum chemistry) and lattice-model calculations [1]. Our findings demonstrate the occurrence of the orientational quasiorder of the water dipoles which become parallel to the tube axis around 150 K [1] and the same reorientation for ammonia dipoles at temperatures below 100 K [2].

We discuss further this temperature-driven quasiphase transition performing more quantum chemical calculations to obtain optimal geometry and charges in the system water/ammonia molecules and SWCNT. Using these results we suggested a simple lattice model to reproduce the properties of the one-dimensional confined finite arrays of water/ammonia molecules. This lattice model takes into account not only the short-range and long-range interactions but also the restricted rotations in a narrow tube, and both ingredients provide an explanation for a temperature-driven orientational ordering of the water/ammonia molecules, which persists within a relatively wide temperature range.

Our theoretical studies were stimulated by experiments of X.Ma et al. on temperature dependence of photoluminescence spectra of water-filled (6,5) SWCNTs [3].

1. M. Druchok, V. Krasnov, T. Krokhmalskii, T. Cardoso e Bufalo, S. M. de Souza, O. Rojas, and O. Derzhko. Toward a quasiphase transition in the single-file chain of water molecules: Simple lattice model// *J. Chem. Phys.* –2023. –Vol.158. –P.104304.
2. M. Druchok, V. Krasnov, T. Krokhmalskii, and O. Derzhko. One-dimensionally confined ammonia molecules: A theoretical study// *Journal of Molecular Liquids.* – 2023. – Vol.387. – P.122633
3. X. Ma, S. Cambre, W. Wenseleers, S. K. Doorn, and H. Htoon. Quasiphase transition in a single file of water molecules encapsulated in (6,5) carbon nanotubes observed by temperature-dependent photoluminescence spectroscopy// *Phys. Rev. Lett.* –2017. –Vol.118. – P.027402.

# Photoelastic parameters of doped potassium sulfate

Stadnyk V.Yo., Shtuka O.V., Shchepanskyi P.A.

*Ivan Franko National University of Lviv, Ukraine*

Recently, the number of works on photoelasticity (piezo- and elasto-optic effects) in crystals of different symmetry classes has increased significantly, which is caused by the search for new optical materials with high acousto-optical (AO) efficiency.

Here, we study the photoelastic properties of potassium sulfate crystals (PS) with manganese admixture  $K_2SO_4:Mn^{2+}$  in order to calculate the components of the piezo-optical coefficients (POC) matrix, elasto-optic coefficients (ELOC) and estimate the AO efficiency of these crystals. To measure the POC  $\pi_{im}^0$ , a polarization-optical method was used, which is based on the interference of light rays that passed through the polarizer-crystal-analyzer system. When the mechanical load  $\sigma_m$  is applied, the interference extrema are shifted, which is observed in the focal plane of the spectral device (DFS-8 spectrograph).

A comparison of the coefficients  $\pi_{im}^0$  of pure and impurity crystals indicates their slight decrease ( $\Delta\pi_{im}^0 \sim 5..9$  Br), which indicates an increase in the mechanical stiffness of impurity crystals. A feature of the  $\pi_{im}^0$  behavior of impurity crystals of potassium sulfate is their significant dispersion, while the character of the dispersion  $d\pi_{im}^0/d\lambda < 0$  corresponds to the dispersion of the refractive indices  $dn_i/d\lambda < 0$ . Different signs and spectral changes of  $\pi_{im}^0$  indicate that the influence of uniaxial stress along the crystallographic directions  $X$ ,  $Z$ , and  $Y$  leads to a different nature of changes in the induced  $\Delta n_i$  of the PS crystal.

Using the obtained experimental changes of  $\pi_{im}^0(\lambda)$ , as well as the known Pockels relations for piezo-birefringence of rhombic crystals, the absolute piezo-optic coefficients  $\pi_{im}$  of  $K_2SO_4$  impurity crystals were estimated at room temperature and for a wavelength of 632.8 nm. In general, the piezo-optic effect of impurity crystals of potassium sulfate is sufficiently large in terms of the  $\pi_{11}$ ,  $\pi_{22}$ , and  $\pi_{12}$  principal POCs.

The estimated AO efficiency of the impurity crystal of potassium sulfate based on elasto-optic coefficients is commensurate with the corresponding for such known AO materials as lithium niobate, lead molybdate, calcium tungstate. Therefore, potassium sulfate crystals, taking into account their short-wave limit of the transparency region of  $\sim 170$  nm, can be used for AO modulation of ultraviolet radiation.

*Acknowledgments:* The study was performed within the framework of the project 2020.02/0211 of the National Research Foundation of Ukraine “Experimental and theoretical study and prediction of the photoelastic properties of crystalline materials for devices of electromagnetic radiation control”.

# Study of fluid H<sub>2</sub> under high pressure: A Generalized collective mode approach

Ilenkov I.-M.<sup>1</sup>, Bryk T.<sup>1,2</sup>

<sup>1</sup>*Institute for condensed matter physics of the National academy of Sciences, Lviv, Ukraine*

<sup>2</sup>*Lviv Polytechnic National University, Lviv, Ukraine*

It is well known [1] that fluid hydrogen, at low pressure, exists in a molecular form. However, as the pressure and temperature increase, molecular hydrogen H<sub>2</sub> undergoes a transition to the atomic state. While at moderate pressure (10<sup>2</sup> – 10<sup>4</sup> bar), the dissociation temperature is approximately equivalent to the molecular bonding energy (~ 4.5 eV), this range is well beyond experimental scope, the dissociation at moderate temperatures (~ 1000 K, which occurs at 1-100 GPa) is of greater interest due to the inherent complexity of atoms' motion. Namely, the separation of the internal degrees of freedom and many-particle interactions disappear, thus leading to the dissociation and subsequent metallization of the system. The Generalized Collective Mode (GCM) approach is particularly valuable for our system analysis, as it can differentiate the contributions from different relaxing and propagating modes to the time correlation functions.

Previously, we conducted AIMD simulations of 500 H<sub>2</sub> molecules at 2500 K and a pressure ranging from 2 to 100 GPa. The trajectories and velocities obtained from these simulations were used to calculate density-density and current-current correlation functions. Additionally, we introduce a smeared step function of the distance, which, being used as a prefactor at the density of molecular units, can describe separately molecular H<sub>2</sub> and dissociated H as two different dynamic variables.

The sets of N = 5 and 7 dynamic variables were applied to derive the generalized hydrodynamic matrix T(k) for the GCM analysis of collective dynamics in fluid H within the pressure-induced molecular-atomic fluid transition region:

$$T(k) = F(k, t = 0) \tilde{F}^{-1}(k, z = 0)$$

Here,  $F(k, t = 0)$  and  $\tilde{F}^{-1}(k, z = 0)$  are N × N matrices of static correlation functions and Laplace-transformed time correlation functions in Markovian approximation. Eigenmodes associated with both purely real and complex-conjugated pairs of eigenvalues corresponded to relaxation and propagating processes in the studied fluid in the pressure-induced molecular-atomic fluid transition region.

1. J. M. McMahon, M. A. Morales, C. Pierleoni, D. M. Ceperley. *The properties of hydrogen and helium under extreme conditions*// Rev. Mod. Phys.-2012-84, 1607

# Effect of metal deposited nanoparticles on microstructure and shear strength of lead-free solder joints

Yu. Plevachuk<sup>1,2\*</sup>, V. Poverzhuk<sup>1</sup>, P. Švec Sr<sup>2</sup>, P. Švec<sup>2,3</sup>, D. Janickovic<sup>2</sup>,  
L. Orovcik<sup>4</sup>, O. Bajana<sup>4</sup>

<sup>1</sup> Department of Metal Physics, Ivan Franko National University of Lviv, Lviv (Ukraine)

<sup>2</sup> Institute of Physics, Slovak Academy of Sciences, Bratislava (Slovakia)

<sup>3</sup> Centre of Excellence for Advanced Materials Application, Slovak Academy of Sciences, Bratislava (Slovakia)

<sup>4</sup> Institute of Materials and Machine Mechanics, Slovak Academy of Sciences, Bratislava (Slovakia)

The rapid development of the electronic industry and the corresponding requirements for the miniaturization of solder joints require the development of new lead-free solders (PbS) with improved thermophysical and mechanical properties [1]. Sn-Ag-Cu (SAC) ternary alloys of eutectic or near-eutectic compositions are considered the most promising and are widely used as solder materials, therefore they require constant improvement of electrical and thermal conductivity, thermal resistance, fatigue and creep resistance, yield strength, etc.

To improve the properties and strengthen the base solder matrix, various nano-sized admixtures, in particular ceramic and carbon, are added [2]. In contrast to metal nanoparticles, they are non-wettable by metal melts. To solve this problem, metallic coatings is applied to their surface to form core-shell structures and to improve adaptation to the solder matrices. As a result, the metal-coated layer forms a strong “bridge” that reacted with the LFS matrix to form an intermetallic layer during soldering. Another important requirement for the LFS application is their reliability in a wide range of operating temperatures, including sub-zero temperatures. In this work, the effect of carbon nanotubes, carbon nanospheres, ceramic oxide admixtures coated with metal nanoparticles on the microstructure and properties of the SAC-based solder joints was studied in a wide temperature range.

## Acknowledgment

The work was supported by by the Office of Government of Slovakia, project no. 09I03-03-V01-00047; the Slovak Scientific Grant Agency under grant nos. VEGA 1/0389/22 and VEGA 2/0144/21; by the SRDA project APVV SK-UA-21-0076; by Ministry of Education and Science of Ukraine, projects nos. 0122U002643, 0122U001521; the study was performed during the implementation of the project Building-up Centre for advanced materials application of the Slovak Academy of Sciences, ITMS project code 313021T081 supported by Research & Innovation Operational Program funded by the ERDF.

1. S. Cheng, C.M. Huang, M. Pecht. *Microelectron Reliab.*, vol.75 (2017), pp. 77-95.
2. M. Li, L. Zhang, N. Jiang, L. Zhang, S. Zhong, *Mater. Des.*, vol. 197 (2021) pp.109224 (2-34).



# **Structural features of thermal expansion of metallic melts.**

**Liudkevych U. I.**

*Andrei Krupynskyi Lviv Medical Academy, Ukraina*

Thermophysical properties of metal melts are current topics of research in modern physics and materials science. Compared to solid alloys, the mechanism of thermal expansion in the liquid state, and especially its relationship with the short-range structure, remain poorly understood. To date, there are no systematic studies that would reveal this problem, and therefore further studies of the mechanism of thermal expansion of melts will contribute to the development of fundamental knowledge about the liquid state of matter.

This work consists the results on studying of temperature variation of structure parameters features in liquid metals In, Sn, Bi, Ga and their alloys (intermetallics InBi, eutectics Bi-Sn and inmiscible melt Ga-Bi). The short range order structure has been studied by means of X-ray diffraction and with use of computer method- Reverse Monte-Carlo simulation. It is proposed to use the temperature dependences of structure parameters, obtained from atomic distribution functions, in order to calculate the thermal expansion coefficient in liquid state and to clarify the thermal expansion mechanism. Temperature dependences of thermal expansion coefficient, calculated from structure data, are analyzed and compared with ones, obtained from experimental data on density that results in conclusion about dominant influence of free volume on kinetics of thermal expansion in metallic melts. It is shown that such temperature dependences reveal the anomalous behavior, which is related with structure transformation in liquid state. Most significant influence of free volume is observed within temperature ranges, where thermal expansion coefficient is negative.

The studying of temperature dependences and calculated thermal expansion coefficients in binary melts shown that individual thermal expansion features of constituent elements are not revealed in melts that is due to formation of chemically ordered clusters with another short range order. Preferred interaction of unlike kind atoms in binary InBi molten alloys significantly transforms the short range of components as well as tendency to like kind atoms interaction in  $\text{Sn}_{57}\text{Bi}_{43}$  and  $\text{Ga}_{70}\text{Bi}_{30}$  melts such changes influence the thermal properties in binaries under investigation. Diffraction data are confirmed by results of computer simulation, which was carried out with help of Reverse Monte-Carlo method.

# Surface tension of equiatomic InBiGaSn and InBiGaSnCu metallic melts

Ovsjanyk R. Ye., Mudry S. I., Bilyk R. M.

*Ivan Franko National University of Lviv, Ukraine*

High-entropy alloys (HEAs) are attracting much attention from researchers because of their unique microstructure and properties, which can be used in a variety of applications. These alloys are highly resistant to corrosion, mechanical stress, and high temperatures, which is making them promising materials for creating various electronic devices such as diodes, transistors, solar panels, and others. In order to further explore and fully understand these materials, it is important to study their other properties, particularly the surface properties. The surface tension of HEAs is a complex property that can be challenging to accurately predict without experimental data, which is why obtaining such data is a high priority for further research in this field.

In our work the surface tension of each alloy was measured using the sessile drop method. The samples were of a higher purity (99.995%) and were heated in a chamber with an inert atmosphere of argon, reaching up to 1400 K with isothermal exposure at reference points every 15 minutes, with a temperature increment of 40 K. A special digital camera was used to photograph the profile of each drop. After computer image processing, a data file containing the temperature dependencies of surface tension was obtained.

In general, the molten equiatomic InBiGaSnCu melt exhibits relatively low surface tension compared to most of its pure components. The same can be said for the four-component equiatomic InBiGaSn alloy. For both investigated melts, the surface tension near the melting point is about 450 mN/m. In these melts, Bi has the lowest surface tension. This observation, along with the obtained X-ray structure data in both liquid and solid states, leads us to conclude that Bi acts as a surfactant in the liquid state of these multicomponent equiatomic metallic melts. This means the presence of absorption processes in the liquid state, leading to a non-equilibrium distribution of Bi in the bulk and on the surface, resulting in a higher concentration of Bi on the surface. As well, the addition of Cu, even in a one-fifth concentration of the alloy, does not affect the surface tension, as there is no presence of its element on the surface. We assume that this tendency in surface tension is caused that liquid Cu has the highest value of surface tension in this equiatomic high entropy melt.

## Секція 2

*Теоретичні дослідження невідпорядкованих систем.*

## Thermodynamic quantities of Morse fluids in the supercritical region

I. V. Pylyuk<sup>1</sup>, M.P. Kozlovskii<sup>1</sup>, O.A. Dobush<sup>1</sup>, M.V. Dufanets<sup>2</sup>

<sup>1</sup>*Institute for Condensed Matter Physics of the National Academy of Sciences of Ukraine*

<sup>2</sup>*Ivan Franko National University of Lviv, Ukraine*

The previously proposed analytical approach [1,2], developed to describe the critical behavior of the cell fluid model by taking into account non-Gaussian fluctuations of the order parameter, is applied to the case where the parameters of the Morse interaction potential correspond to alkali metals (sodium and potassium). The critical temperatures, densities, and pressures obtained for sodium and potassium agree with the experimental results. The thermodynamic coefficients (isothermal compressibility, density fluctuations, and thermal expansion) of sodium are investigated in the supercritical temperature region [3]. For this purpose, we use the equation of state obtained in [1] for the cell fluid model. Numerical calculations of thermodynamic coefficients are performed close to the critical point, where carrying out theoretical and experimental research is challenging. The change in compressibility with increasing density at various temperature values is traced. The behavior of density fluctuations approaching the critical point is shown for different temperatures. The variation in the magnitude of the thermal expansion with increasing temperature for different pressure values is illustrated.

The isothermal compressibility and the density fluctuations become enormous when approaching the critical point. Very large values of the isothermal compressibility mean a substantial density sensitivity to tiny pressure fluctuations. For various fixed pressure, we see a decrease in the thermal expansion coefficient with increasing supercritical temperature, which is typical of gases. The thermal expansion coefficient of gases with increasing temperature approaches the value of the thermal expansion coefficient of an ideal gas, which is equal to the reciprocal absolute temperature.

Our approach to simple fluid systems will help to study the critical behavior of multicomponent fluids.

1. M.P. Kozlovskii, I.V. Pylyuk, O.A. Dobush. The equation of state of a cell fluid model in the supercritical region // *Condens. Matter Phys.* – 2018. – Vol. 21. – 43502.
2. I.V. Pylyuk. Fluid critical behavior at liquid – gas phase transition: Analytic method for microscopic description // *J. Mol. Liq.* – 2020. – Vol. 310. – 112933.
3. I. V. Pylyuk, M.P. Kozlovskii, O.A. Dobush, M.V. Dufanets. Morse fluids in the immediate vicinity of the critical point: Calculation of thermodynamic coefficients // *J. Mol. Liq.* – 2023. – Vol. 385. – 122322.

# Pseudo Jahn-Teller cooperative ordering in layered $\text{KEr}(\text{MoO}_4)_2$ induced by a magnetic fields up to 30 T

N. M. Nesterenko<sup>1</sup>, K. Kutko<sup>1</sup>, B. Bernáth<sup>2</sup>, D. Kamenskyi<sup>3</sup>

<sup>1</sup>*B.Verkin Institute for Low Temperature Physics and Engineering of NAS of Ukraine, 47 Nauky Ave., Kharkiv, 61103, Ukraine*

<sup>2</sup>*High Field Magnet Laboratory (HFML – EMFL), Radboud University, Toernooiveld 7 6225 ED Nijmegen, The Netherlands*

<sup>3</sup>*Experimental Physics V, Center for Electronic Correlations and Magnetism, Institute of Physics, University of Augsburg, 86159 Augsburg, Germany  
e-mail: nesterenko@ilt.kharkov.ua*

The  $\text{KEr}(\text{MoO}_4)_2$  is a ‘virtual’ Jahn-Teller (JT) crystal [1], which includes at least 4 JT centers in the elementary cell, pair of them lays in the different layers [2]. In this work we study Zeeman effect in  $\text{KEr}(\text{MoO}_4)_2$  at external magnetic field up to 30T by far infrared (FIR) spectroscopy. FIR spectra of  $\text{KEr}(\text{MoO}_4)_2$  are formed by electronic transitions between the components of the ground multiplet  $^4I_{15/2}$ , which is split in the rhombic crystal field, and by low-energy phonon excitations. Figure 1 shows the behavior of excitations when the external magnetic fields are changed up to 30T ( $\mathbf{H}\parallel a$ ,  $\mathbf{H}\parallel b$ ,  $k\parallel b$ ,  $T=1.4\text{K}$ ).

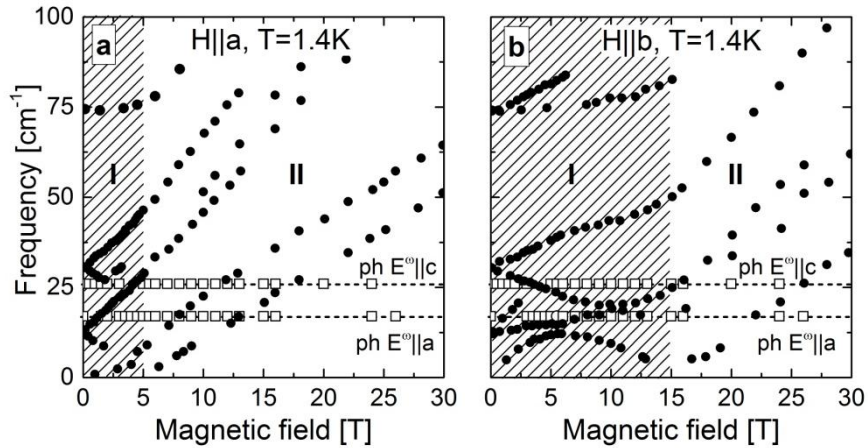


Fig.1. Frequency-magnetic field dependences of low frequencies excitations in  $\text{KEr}(\text{MoO}_4)_2$  ( $T=1.4\text{K}$ ): a –  $\mathbf{H}\parallel a$ ; b –  $\mathbf{H}\parallel b$ . ● – excitations of electronic nature, ◻ - phonon-type excitations. In the regions I and II are observed different behavior of electronic excitations.

From measured spectra follows that in the magnetic field above  $H_{\text{cr}}$  ( $H_{\text{cr1}} \sim 5\text{T}$  ( $\mathbf{H}\parallel a$ ) and  $H_{\text{cr2}} \sim 15\text{T}$  ( $\mathbf{H}\parallel b$ )) the linear dependences are observed for all excitations. In the region below  $H_{\text{cr1}}$  and  $H_{\text{cr2}}$  the magnetic field induces the spatially nonhomogeneously states, which appear in the form of ‘‘anticrossing type’’ behavior of some excitations.

Note, that for  $\mathbf{H}\parallel b$  ( $b$  is perpendicular to layers) the spatially homogeneous state was observed at  $H_{\text{cr2}} = 15\text{T}$  [3]. Considering of the layered structure of  $\text{KEr}(\text{MoO}_4)_2$ , which include two layers changing alternatively along  $b$  axis - erbium and potassium ones (the last one does not sensitive to external magnetic

field), we conclude that the rotations of molybdenum tetrahedrons, surrounding  $\text{Er}^{3+}$  ions, play the significant role in the process of the elastic type ordering. We discuss also the low energy phonon displacements which may lead to the ordering of the local JT distortions.

[1] G.A. Zviagina, A.A. Zviagin, *Fiz. Nizk.Temp.* **26**, 482 (2000).

[2] V.I. Spitsyn, V.K. Trunov, *Docl. Akad. Nauk SSSR*, **185**, 854 (1969).

[3] B. Bernáth, K. Kutko, S. Wiedmann, O. Young, H. Engelkamp, P. C. M. Christianen, S. Poperezhai, L. V. Pourovskii, S. Khmelevskiy, and D. Kamenskyi, *Adv. Electron. Mater.* **8**, 2100770 (2022).

# Bending-induced states in thin layers of van der Waals ferrielectrics

Anna N. Morozovska<sup>1</sup>, Eugene A. Eliseev<sup>2</sup>, Andrii V. Bodnaruk<sup>1</sup>, Nicholas V. Morozovsky<sup>1</sup>, Andrei L. Kholkin<sup>3</sup>, Yulian M. Vysochanskii<sup>4</sup>, Sergei V. Kalinin<sup>5</sup>

<sup>1</sup> *Institute of Physics, National Academy of Sciences of Ukraine,  
46, Prospekt Nauky, 03028 Kyiv, Ukraine*

<sup>2</sup> *Institute for Problems of Materials Science, National Academy of Sciences of Ukraine,  
3, Krjijanovskogo, 03142 Kyiv, Ukraine*

<sup>3</sup> *Computational Sciences and Engineering Division, Oak Ridge National Laboratory, Oak Ridge, Tennessee,  
37831*

<sup>4</sup> *Department of Physics and Materials Research Institute, Pennsylvania State University, University Park,  
Pennsylvania 16802, United States*

<sup>5</sup> *Department of Physics & CICECO – Aveiro Institute of Materials, Campus Universitario de Santiago,  
3810-193 Aveiro, Portugal*

<sup>6</sup> *Institute of Solid-State Physics and Chemistry, Uzhhorod University,  
88000 Uzhhorod, Ukraine*

<sup>7</sup> *Department of Materials Science and Engineering, University of Tennessee,  
Knoxville, TN, 37996, USA*

Using Landau-Ginzburg-Devonshire (LGD) phenomenological approach we analyze the bending-induced re-distribution of electric polarization and field, elastic stresses and strains inside ultrathin layers of van der Waals ferrielectrics on example of  $\text{CuInP}_2\text{S}_6$  (CIPS). The unique aspect of CIPS is the existence of two ferrielectric states, FI1 and FI2, corresponding to big and small polarization values. When the CIPS layer is flat, the single-domain FI1 state is stable in the central part of the layer, and the FI2 states are stable near the fixed edges. With an increase of the layer bending below the critical value, the sizes of the FI2 states near the fixed edges decreases, and the size of the FI1 region increases. When the bending exceeds the critical value, the edge FI2 states disappear being substituted by the FI1 state, but they appear abruptly near the inflection regions and expand as the bending increases. The calculated phase diagrams show that the transition between the FI1 and FI2 states can be induced by the tangential strains created by the rough substrate. The FI1-FI2 transition can significantly reduce the coercive voltage of ferroelectric polarization switching in ultrathin CIPS nanoflakes, which is urgent for their advanced applications. The FI1-FI2 transition is specific for those bended vdW ferrielectrics, which are described by the eighth (or higher) order LGD functional.

[1] A. N. Morozovska, E. A. Eliseev, Y. Liu, et al. Bending-induced isostructural transitions in ultrathin layers of van der Waals ferrielectrics, <https://doi.org/10.48550/arXiv.2305.15247>

Acknowledgements. A.N.M. and A.V.B. acknowledge the support from the National Research Fund of Ukraine (project “Low-dimensional graphene-like transition metal dichalcogenides with controllable polar and electronic properties for advanced nanoelectronics and biomedical applications”, grant application 2020.02/0027). A.L.K. acknowledge support from the European Union’s Horizon Europe (HORIZON) research and innovation programme (PIEZO-2D).

# **Polar and electrophysical properties of the nanostructure “graphene on a Janus compound ultrathin film”**

Anna N. Morozovska<sup>1</sup>, Andrii V. Bodnaruk<sup>1</sup>, and Eugene A. Eliseev<sup>2</sup>,

<sup>1</sup> *Institute of Physics, National Academy of Sciences of Ukraine,  
Pr. Nauky 46, 03028 Kyiv, Ukraine,*

<sup>2</sup> *Institute for Problems of Materials Science, National Academy of Sciences of Ukraine, Krjijanovskogo  
3, 03142 Kyiv, Ukraine*

Using the phenomenological approach we study the charge-polarization coupling in the nanostructure “thin Janus compound film – single-layer graphene”. We evolve the Landau-Ginzburg-Devonshire model of the polar and antipolar ordering in the Janus compound XMY films, which are strongly influenced by the surface and thickness effects, and propose a simple phenomenological description of the polarization behavior in the films. The recently discovered and poorly studied Janus ultrathin layers and films with controllable polar and electronic properties, such as XMY, where M is a transition metal, X and Y are different chalcogenides, are very promising candidates for advanced nanoelectronics and biomedical applications.

Due to the inversion symmetry breaking, XMY are piezoelectric by their nature, because the layer of M-atoms is placed between the layers of different chalcogenides, X and Y. At the same time, the Janus-type piezoelectric polarization of the XMY film influences strongly on the graphene conductivity, and the full correlation between the distribution of polarization and charge carriers in graphene is revealed. In accordance with our modeling, the polarization of the ultrathin XMY films, which can be in the ferroelectric-like or antiferroelectric-like states, determine the concentration of carriers in graphene and can control its field dependence and spatial modulation.

The result can be promising for creation of next generation Si-compatible nonvolatile random access memories and graphene-ferroelectric field-effect transistors, because the working voltages applied to the XMY film (which acts as a piezoelectric gate) can be relatively low (less than 2 V). These low voltages are sufficient to induce the pronounced hysteresis of the graphene charge.

Acknowledgements. A.N.M. and A.V.B. acknowledge the support from the National Research Fund of Ukraine (project “Low-dimensional graphene-like transition metal dichalcogenides with controllable polar and electronic properties for advanced nanoelectronics and biomedical applications”, grant application 2020.02/0027).



# Critical behavior of systems with long-range interactions and structural disorder

Maxym Dudka<sup>1, 2, 3</sup>, Dmytro Shapoval<sup>1, 2</sup>, and Yuriy Holovatch<sup>1, 2, 4, 5</sup>

<sup>1</sup>*Institute of Condensed Matter Physics, National Academy of Sciences of Ukraine, 79011 Lviv, Ukraine*

<sup>2</sup>  $\mathbb{L}^4$  *Collaboration & Doctoral College for the Statistical Physics of Complex Systems, Leipzig-Lorraine-Lviv-Coventry, Europe*

<sup>3</sup>*Lviv Polytechnic National University, 79013, Lviv, Ukraine*

<sup>4</sup>*Centre for Fluid and Complex Systems, Coventry University, Coventry CV1 5FB, UK*

<sup>5</sup>*Complexity Science Hub Vienna, 1080 Vienna, Austria*

Examination of the impact of structural inhomogeneity on the universal characteristics of physical systems is of significant relevance, as a majority of materials exhibit some degree of disorder [1]. In magnetic systems, structural inhomogeneity can manifest in diverse ways, resulting in distinct alterations in critical behavior. The degree of structural disorder is particularly crucial, as a pronounced disorder can introduce frustrating effects and potentially result in the absence of long-range magnetic order [2]. Systems with long-range interactions display unique properties compared to those with short-range interactions and have extensive applications in various fields [3]. Even weak long-range interactions can have a considerable influence on critical properties [4].

Therefore we use an  $n$ -vector model in  $d$ -dimensional space to investigate how do the structurally disordered systems (e.g. quenched weakly diluted magnets) with long-range interactions behave near critical points. We assume that the interactions decay as a power-law  $x^{-(d+\sigma)}$  with distance  $x$  and a control parameter of the interaction decay  $\sigma$ . In regular lattices, the critical behavior of the  $n$ -vector model is governed by the global parameters  $d$ ,  $n$ , and  $\sigma$ , and depending on their values, the model may exhibit a low-temperature long-range magnetic order that emerges as a second-order phase transition. The transition to the magnetically-ordered phase is characterized by universal features and belongs to a certain universality class. Our goal is to show how these universal features change when considering a disordered lattice structure, such as the one imposed by dilution. In particular, this model is known to belong to the new universality class induced by dilution in some region of the  $(n, d, \sigma)$  parameter space [5]. We apply field-theoretic renormalization group approach calculating the  $\beta$ -functions and fixed points coordinates in the three-loop approximation and providing analysis of critical exponents. Employing a perturbative  $\varepsilon = 2\sigma - d$  - expansion technique, we derive the correlation length critical exponent  $\nu(\sigma, d)$  of the  $n$ -vector model with long-range interactions. To obtain precise numerical

values, we further employ resummation methods, enhancing the accuracy of our results.

M.D. and D.S. acknowledge the support of the U. S. Department of Energy (DOE), Office of Science, Basic Energy Sciences, Materials Science and Engineering Division, under Award No. DE–SC0013599

1. *Order, Disorder and Criticality. Advanced Problems of Phase Transition Theory*. edited by Yu. Holovatch. Vols. 1–7 (World Scientific, Singapore, 2004–2022)
2. *Phase Transitions and Critical Phenomena*, edited by C. Domb and J. L. Lebowitz (Academic, London, 1983)
3. *Dynamics and Thermodynamics of Systems with Long-Range Interactions*, edited by T. Dauxois, S. Ruffo, E. Arimondo, M. Wilkens, Lect. Not. in Phys. **602** (Springer-Verlag, New York, 2002)
4. D. Mukamel, *Notes on the statistical mechanics of systems with long-range interactions* (2009) [arXiv: 0905.1457]
5. D. Shapoval, M. Dudka, Yu. Holovatch, *Low Temp. Phys.* **48** (2022) 1049

# Phenomenological generalizations of conventional quantum statistical distributions

A. Rovenchak, B. Sobko

*Ivan Franko National University of Lviv, Ukraine*

The aim of the talk is to elucidate potential mathematical simplifications in handling some real-world physical systems. This might be achieved by transferring certain system properties, such as interparticle interactions, finite number of particles, etc., to parameters associated with fractional (or intermediate) statistics. These types of fractional statistics emerge as substitutes for conventional bosonic or fermionic ones.

One approach to achieve this entails deriving the relevant parameters from microscopic considerations, which would be the most direct, though technically much more complicated, method. However, there exists also a simpler detour. It involves phenomenological generalizations of expressions for occupation numbers, introducing a few unknown parameters. Subsequently, these newly introduced parameters are linked to certain properties of the system under consideration [1–3]. Such an approach allows for an effective description of a real physical system as an ideal system obeying certain fractional statistics.

1. B. Sobko and A. Rovenchak. Effective modeling of physical systems with fractional statistics // *Low Temp. Phys.* 2022. Vol. 48, No. 8. P. 621–627. <https://doi.org/10.1063/10.0012649>
2. Rovenchak and B. Sobko. Fugacity versus chemical potential in nonadditive generalizations of the ideal Fermi-gas // *Physica A.* 2019. Vol. 534. Article 122098. <https://doi.org/10.1016/j.physa.2019.122098>
3. Rovenchak. Weakly nonadditive Polychronakos statistics // *Phys. Rev. A.* Vol. 89, No. 5. Article 052116. <https://doi.org/10.1103/PhysRevA.89.052116>

# Phase behavior of ionic liquids in ultranarrow imhomogeneous slit pore

Maxym Dudka<sup>1, 2, 3</sup>

<sup>1</sup>*Institute of Condensed Matter Physics, National Academy of Sciences of Ukraine, UA -- 79011 Lviv, Ukraine*

<sup>2</sup>  $\mathbb{L}^4$  *Collaboration & Doctoral College for the Statistical Physics of Complex Systems, Leipzig-Lorraine-Lviv-Coventry, Europe*

<sup>3</sup>*Lviv Polytechnic National University, UA --79013, Lviv, Ukraine*

Confined ionic liquids exhibit exciting physics and play an essential role in modern technology, particularly in capacitive energy storage and conversion. The narrow conducting confinements cause exponential screening of the electrostatic interactions between ions, allowing the development of models with short-range interactions that can provide analytical insights into the charge storage. In this contribution, a lattice model for ultranarrow slit pores admitting a single layer of ions is discussed. It can be mapped onto the well-known three state Blume-Capel model and can be solved analytically within the Bethe-lattice approximation for the case of nearest neighbours interactions [1]. Then phase behaviour and pore charging in terms of pore ionophilicity, interionic interactions, and applied electrode potential can be analysed. The obtained phase diagram includes the lines of first- and second-order, direct and re-entrant phasetransitions, manifested by singularities in the capacitance-voltage dependence [2]. The imhomogeneous structure of the pore behaviour is modelled by introducing random ionophobicity. The results show considerable influence of randomness of phase diagram, which is dependent in this case on the degree of disorder.

This research is supported by bilateral project between Ministry of Education and Science of Ukraine and Polish National Agency for Academic Exchange (NAWA) as well as U. S. Department of Energy (DOE), Office of Science, Basic Energy Sciences, Materials Science and Engineering Division, under Award No. DE-SC0013599

[1] M. Dudka, S. Kondrat, A.A. Kornyshev, G. Oshanin, *J. Phys.: Condens. Matter* **28**, 464007 (2016).

[2] Dudka, S. Kondrat, O. Benichou, A. A. Kornyshev, G. Oshanin, *J. Chem. Phys.* **151**, 184105 (2019).

# Плазмони в металевих стрижнеподібних наночастинках із періодично модульованою бічною поверхнею

Коротун А.В.<sup>1,2</sup>

<sup>1</sup>Національний університет «Запорізька політехніка», Україна

<sup>2</sup>Інститут металофізики ім. Г. В. Курдюмова НАН України, Україна

Відомо, що несферичні металеві наночастинки демонструють анізотропні оптичні відгуки, що визначаються, перш за все, їх геометричними особливостями. Так, у металевих нанострижнях можливе збудження двох плазмонних мод. При цьому положенням поздовжнього ППР можна керувати шляхом зміни аспектного відношення. Крім того, металеві нанострижні демонструють також істотне підсилення електричного поля у своїх кінцях при резонансному збудженні. Також потрібно відзначити наявність розбіжностей між теоретичними та експериментальними спектрами екстинкції нанострижнів, причиною якої, на думку авторів [1] є неврахування періодичної модуляції поверхні та наявність на півсфер на кінцях нанострижнів. У зв'язку з цим дослідження оптичних властивостей циліндрів і сфероциліндрів із періодичною модуляцією бічної поверхні є актуальною задачею.

Для знаходження поляризованості використовуватимемо модель еквівалентного витягнутого сфероїда та квазістатичне наближення, в рамках якого потенціал для областей всередині ( $i=1$ ) і зовні ( $i=2$ ) сфероїда визначається розв'язками рівняння Лапласа

$$\Delta\varphi_i = 0 \quad (1)$$

з граничними умовами рівності потенціалів і нормальних складових електричних полів на поверхні сфероїда  $S$ :

$$\varphi_1|_S = \varphi_2|_S, \quad \hat{\epsilon}(\omega) \frac{\partial\varphi_1}{\partial\mathbf{n}} \Big|_S = \epsilon_m \frac{\partial\varphi_2}{\partial\mathbf{n}} \Big|_S. \quad (2)$$

У формулі (2)  $\epsilon_m$  – діелектрична проникність оточуючого середовища;  $\hat{\epsilon}(\omega)$  – діелектричний тензор матеріалу сфероїда.

Розв'язання задачі (1) – (2) дозволяє за умови малої глибини модуляції ( $a/r_0 \ll 1$ ) отримати частотні залежності діагональних елементів тензора поляризованості і, відповідно, перерізу екстинкції. Результати розрахунків свідчать про близькість теоретичних спектрів екстинкції для сфероциліндрів із періодично модульованою бічною поверхнею до експериментальних спектрів.

1. C. Pecharrómán, J. Pérez-Juste, G. Mata-Osoro, L.M. Liz-Marzán, P. Mulvaney. Redshift of surface plasmon modes of small gold rods due to their atomic roughness and end-cap geometry // Phys. Rev. B. – 2008. - Vol.77. – id. 035418.

## Dicke model as a disordered system

Lyagushyn S.F., Sokolovsky A.I.

*Oles Honchar Dnipro National University, Ukraine*

A system of two-level atoms described by the Dicke Hamiltonian can be a source of a short coherent emission pulse [1]. Such superradiance phenomenon is possible for both electromagnetic and acoustic emission [2], and its importance for theory development and practice is out of doubts. The macroscopic filling of the resonant boson mode evidences the long order in the system of emitters. Initially, their emission is not correlated in phase and direction. The separation of modes to be amplified is ensured by the shape of emitter subsystem and the exciting pulse polarization. The spatial distribution of an individual emitter radiation is determined by the vector  $\mathbf{d}_a$  – dipole moment of the operation transition of  $a$ -th emitter wherein the full Hamiltonian includes the term  $-\sum_a (\mathbf{d}_a \cdot \mathbf{E})$ . The correctness of such quantum approach has been substantiated. Operators  $\mathbf{d}_a$  are represented via Pauli matrices in quasispin space and have an inevitable phase uncertainty like collective quasispin operators  $R^\pm$  in thermodynamical investigation of Dicke model. In further analysis the uncertainty is eliminated due to using averages  $\langle R^+ R^- \rangle$  [1, 4]. Herewith the expression  $\mathbf{d} = d\mathbf{n}$  where  $d$  is a quasispin operator and  $\mathbf{n}$  is a random unit vector in the real space should be applied. One can see that such model is analogous to spin glass, and in this framework the material equations for a medium of emitters and evolution equations considering field correlations were constructed [5], and the picture of correlation development in terms of waves in medium was created [6].

1. N.Bogolyubov (Jr.), A.Shumovsky. Superradiance. -Dubna: JINR, 1987. - 88 p. (in Russian)
2. V.Golenishchev-Kutuzov, V.Samartsev, B.Khabibullin. Pulsed optical and acoustic coherent spectroscopy. -Moscow: Nauka, 1988. -224 p. (in Russian)
3. K.Hepp, E.Lieb. Equilibrium statistical mechanics of matter interacting with the quantized radiation field// Phys. Rev. A. -Vol. 8. -P.2517-2525.
4. S.Lyagushyn, A.Sokolovsky. Order parameters in Dicke model// J. of Physics&Electronics. -2022. -Vol.30(2). -P.15-22.
5. S.Lyagushyn, A.Sokolovsky, S.Sokolovsky. Kinetics of electromagnetic field in nonequilibrium medium// J. of Physics&Electronics. -2019. - Vol.27(2). -P.17-28.
6. S.Lyagushyn, A.Sokolovsky. Dispersion equation for electromagnetic waves in a Dicke system // J. of Physics&Electronics. -2022. -Vol.30(1). - P.31-38.

# **Modeling of the electrical response of random heterogeneous systems: A hard core – inhomogeneous penetrable shell model**

Sushko M.Ya.

*Mechnikov National University, Odesa, Ukraine*

The study of the effective electrical properties (conductivity, permittivity etc.) of random systems is a challenging many-particle problem; typically, it is approached by using a number of poorly justified and actually one-particle approximations. We discuss a many-particle model where the properties of a real random system are assumed to be equivalent to those of a collection of particles with the hard-core–inhomogeneous-penetrable-shell morphology. The key suggestions of the model are as follows: (1) the complex permittivity of the shells can be modeled so as to account for major mechanisms in the real system; (2) definite rules of dominance can be imposed on the overlapping structural units to reflect microstructural alterations in the system with filler concentration variations; and (3) our original compact group approach for electrodynamic homogenization of random systems can be used to effectively evaluate many-particle polarization and correlation contributions to the desired quantity (say, the effective electrical conductivity) without in-depth assumptions. As a result, we manage to derive integral relations for the desired quantity; they are rigorous in the static limit.

We demonstrate the specific features of the theory and its capability to recover experiment by applying the results obtained to a number of various physical systems, which include: dispersions of graded particles [1]; composite solid electrolytes [2]; polymeric composite electrolytes [3]; and latex suspensions in aqueous electrolyte with high ionic strength [4]. In addition, we give an interpretation of our results in application to polymer–metallic-powder composites with another – segregated – type of the filler distribution.

1. M.Ya. Sushko. Effective dielectric response of dispersions of graded particles// *Phys. Rev. E.* -2017. Vol.96. -P.062161 (8 pp).
2. M.Ya. Sushko, A.K. Semenov. Rigorously solvable model for the electrical conductivity of dispersions of hard-core–penetrable-shell particles and its applications// *Phys. Rev. E.* -2019. Vol.100. -P.052601 (14 pp).
3. M.Ya. Sushko, A.K. Semenov. A mesoscopic model for the effective electrical conductivity of composite polymeric electrolytes// *J. Mol. Liq.* - 2019. Vol.279. -P.677-686.
4. M.Ya. Sushko, S.D. Balika. Effect of the electrical double layer on the electrical conductivity of suspensions// *Phys. Scr.* -2023. Vol.98. - P.015812 (12 pp).

# **Thermal Conductivity Analysis for Disordered Crystals: contemporary view**

Horbatenko Yu. V., Krivchikov A. I., Romantsova O. O., Koroluyk O. A.

*B. Verkin Institute for Low Temperature Physics and Engineering of NAS of Ukraine,  
47 Nayky Ave., Kharkiv 61103, Ukraine  
email:horbatenko@ilt.kharkov.ua*

Thermal property`s investigations are an important area of modern material science – it stimulates the development of new functional materials with specified physical and chemical properties. As usual, thermal conductivity of ordered solids sometimes consider in terms of phonon gas model, where phonons seem to quasiparticles, which take part in scattering processes in crystal lattice. The quasi-particle description of heat transfer makes senseless for disordered solids because of lack of the periodicity, when mean free path (MPF) of phonons becomes comparable with phonon wavelength. Also, the character of temperature dependences of the thermal conductivity of disordered crystals, especially at low temperatures, differs significantly for their crystalline analogs. Therefore the different phenomenological models - the Cahill-Pohl model [1], the Tunnel Model (TM) [2-3], and its extension - Soft Potential Model (SPM) [4], are often used to describe the thermal conductivity of the disordered solids at lowest temperatures. The thermal conductivity of weakly disordered systems can be calculated using perturbation theory [5], and the Allen-Feldman approach was used to characterize atomic vibrations in amorphous Si [6].

Finally, we discuss unified theory of thermal transport, which proposed by Marzari-Mauri [7], and declares that heat transfer in solids has two channels - quasi-particles and wave-tunneling: the first one dominates in ordered crystals, and the second one - in disordered solids. We show a procedure for processing and further analysis of the thermal conductivity data for various disordered and amorphous materials, such as molecular, semiconductive, clathrate compounds, skutterudites, ceramics, and polymers in a wide temperature range. All of these data can be approximated by an Arrhenius-type expression.

1. D.G.Cahill and R.Pohl. Heat flow and lattice vibrations in glasses // Solid State Commun. -1989. - V. 70, № 10. - P. 927-930.
2. P.W. Anderson, B.I. Halperin, and C.M. Varma. Anomalous low-temperature thermal properties of glasses and spin glasses // Philos. Mag. - 1972. - V. 25, № 1. - P. 1-9.
3. P.Sheng and M.Zhou. Heat Conductivity of Amorphous Solids: Simulation Results on Model Structures // Science. - 1991. - V. 253, № 5019.- P. 539-542.
4. M. A. Ramos and U. Buchenau. Beyond the Standart Tunneling Model: The Soft-Potential Model // Tunneling Systems in Amorphous and Crystalline Solids. - Springer Berlin Heidelberg, 1998. - P. 527-569.



5. J. Garg, N. Bonini, B. Kozinsky [et al.]. Role of Disorder and Anharmonicity in the Thermal Conductivity of Silicon-Germanium Alloys: A First-Principles Study // Phys. Rev. Lett. - 2011. - V.106, №4. - P. 045901-1-045901-4.
6. P. B. Allen, J. L. Feldman, J. Fabian [et al.]. Diffusons, locons and propagons: Character of atomic vibrations in amorphous Si // Philos. Mag. - 1999. - V. 79, № 11-12. - P. 1715-1731.
7. [M. Simoncelli](#), [N. Marzari](#), [F. Mauri](#). Unified theory of thermal transport in crystals and glasses // Nature Physics. - 2019. - V. 15, № 8. - P. 809-813.

**Acknowledgments:** This work has received funding from the National Research Foundation of Ukraine (NRFU project № 2020.02/0094).

# Entanglement Entropy of Free Disordered Fermions

Pastur L.A.

*Institute for Low Temperature Physics and Engineering, Kharkiv, Ukraine*

We consider the macroscopic system of free lattice fermions and we are interested in the entanglement entropy of a large block of size  $L$  of the system viewing the rest of the system as the macroscopic environment of the block. The entanglement entropy is a widely used quantifier of quantum correlations between the block and its environment. We begin with the summary of known results on the large- $L$  asymptotic behavior of the entanglement entropy for various translation invariant systems, where there are two basic asymptotics known as the area law *and the enhanced (or violated) area law*.

We then show that in the disordered case and for the Fermi energy belonging to the localized spectrum of the one-body Hamiltonian the entanglement entropy follows the area law for all typical realization of the disorder and any dimension and we give an explicit formula for the entanglement entropy via the Fermi projection of the one-body Hamiltonian of the system. As for the enhanced area law, it turns out to be possible for certain special values of the Fermi energy in the one-dimensional case.

# Phase behavior of a binary mixture with Curie-Weiss interaction

M. P. Kozlovskii<sup>1</sup>, O. A. Dobush<sup>1</sup>

<sup>1</sup>*Institute for Condensed Matter Physics of the National Academy of Sciences of Ukraine*

We consider a model of a continuous, binary system within the framework of the grand canonical ensemble. The particles interact via the Curie-Weiss potential, which contains attractive and repulsive components. The values of the interaction parameters of each species are different, which ensures the asymmetry of the mixture. Moreover, the interaction between particles of distinct sorts is taken into account. We calculated the grand partition function of the model and obtained critical values of the intensive properties for specific values of the interaction parameters. The phase behaviour of such a model, namely the first-order phase transitions, is analysed in a wide range of density and temperature.

This work was supported by the funds of a grant of the National Academy of Sciences of Ukraine within the framework of scientific projects of research laboratories/groups for young scientists No 07/01-2023(4). We thank the Armed Forces of Ukraine for providing security to perform this work.

## Секція 3

*Аморфні сплави. Синтез, структура та фізичні  
властивості.*

# **Nanocrystallization of amorphous alloys under the action of irradiation with argon ions**

Tsaregradskaya T.L., Ovsienko I.V., Kozachenko V.V.,

Kuryliuk A.M., Saenko G.V., Turkov O.V.

*Taras Shevchenko National University of Kyiv, Ukraine*

Irradiation of amorphous alloys with ion beams is a promising technology for obtaining new materials with specified properties. The aim of the research is to analyze the possibility of obtaining an amorphous nanostructured state from the original amorphous state by ion irradiation.

The processes of phase formation in the  $\text{Fe}_{75}\text{Mo}_5\text{Si}_6\text{B}_{14}$  amorphous alloy under the influence of argon ion irradiation have been investigated using the methods of highly sensitive dilatometry, microhardness measurements, and electron microscopy. The surface of the amorphous alloy was treated with argon ions at a voltage of 1 kV at the anode and a current through the sample of 1 mA. The surface morphology of the amorphous alloy treated with argon ions was studied using a LensSEI scanning electron microscope.

The structure of amorphous alloys is characterized by the presence of frozen-in centers of crystallization. The condition of thermodynamic equilibrium of the system “amorphous matrix – frozen-in centers of crystallization” is equality  $\Delta\mu_i = 0$ , when the condition  $\Delta\mu_i < 0$  is fulfilled, the crystal nuclei dissolve in the amorphous matrix, and when the condition  $\Delta\mu_i > 0$  is fulfilled, the frozen-in centers of crystallization in the amorphous phase grow [1]. Radiation-induced crystallization of amorphous alloys has significant differences compared to thermally induced crystallization, which is manifested in a decrease in the temperature threshold.

It is shown that the phenomenon of nanocrystallization is not observed during exposure to ion irradiation for up to 30 minutes, on the contrary, the frozen-in centers of crystallization dissolve in the stability by 25 K and an increase in microhardness by 8.2%, thus, strengthening of the alloy, which may indicate the formation of an amorphous nanocrystalline state. This fact is confirmed by SEM studies of the surface morphology of the amorphous alloy: the size of the frozen amorphous matrix. With an irradiation time of 45 minutes, there is a decrease in thermal centers of crystallization increased after irradiation with argon ions for 45 minutes. This is explained by the creation of thermodynamic conditions for the growth of frozen-in crystallization centers when the temperature in the regions of the ion tracks reaches threshold values where the condition  $\Delta\mu_i > 0$  is fulfilled.

1. V. Lysov, T. Tsaregradskaya, O. Turkov, G. Saenko. Influence of thermal treatment on phase formation processes in amorphous alloys // Springer Proceedings in Physics.- 2018. – 210. - 341.

# Ga-Ge-Te alloys: structural properties

Popovych M.V., Stronski A.V., Shportko K.V.

*I V.Lashkaryov Institute of Semiconductor Physics NAS Ukraine, Kyiv, Ukraine,  
niva94@ukr.net*

GaGeTe glasses have many applications in phase change-type optical memory, far-IR optics, and sensors [1]. The structural properties of chalcogenide glasses and their correlations with various characteristics and processes, including photoinduced ones are important for their practical use. The doping by Ga of GeTe alloys change crystallization timings and room temperature stability. Change of structural properties with the composition, The better understanding of the correlations between structural and macroscopic properties of Ga-Ge-Te glasses can help in optimization of the properties, sensitivity and relief formation processes of various composite nanomultilayer structures based on such chalcogenide glasses.

In the present report the amorphous Ga-Ge-Te alloys have been studied by X-ray diffraction. Studied bulk Ga-Ge-Te alloys were prepared by the conventional melt quenching technique. Composition was controlled using EDX. X-ray diffraction patterns of samples were recorded with use of the X-ray diffractometer with Bragg–Brentano geometry, using Cu Ka radiation 1.54178 Å and mounted graphite monochromator for a diffracted beam. The diffraction data were collected in the range of scattering vector magnitudes  $Q$  between 0.4 and 8 Å,  $Q = 4\pi \sin \theta / \lambda$ . All samples were examined in transmission geometry. All the X-ray experiments were performed at ambient temperature. The experimental X-ray diffraction patterns were used for calculations of radial distribution functions which have given the positions of the nearest-neighbour bond length  $r_1$  and second-neighbour bond length  $r_2$  (see Table).

composition	$r_1, \text{Å}$	$r_2, \text{Å}$	$\Theta, ^\circ$
Ga <sub>7.9</sub> Ge <sub>11.49</sub> Te <sub>80.61</sub>	2.65	4.44	114°
Ga <sub>11.7</sub> Ge <sub>14.1</sub> Te <sub>74.2</sub> [1]	2.67	4.27	106°

Similar  $r_1$  values were observed for Ga-Ge-Te glasses of other compositions known from reference literature. The calculated bond angle  $\Theta$  values are also in good agreement with other published data on GaGeTe alloys

The better understanding of the correlations between structural and macroscopic properties and the information on the short-range order structure of Ga-Ge-Te chalcogenide glasses is needed.

1. Popovych M.V., Stronski A.V., Shportko K.V. Structural properties of Ga<sub>11.7</sub>Ge<sub>14.1</sub>Te<sub>74.2</sub> alloys. *Physics and Chemistry of Solid State*. 2022. V. 23, No. 4 pp. 830-835.

# Effect of lattice disorder on charge transfer in $\text{PbMoO}_4$ single crystals

Bochkova T.M.<sup>1</sup>, Krivchenko A.Yu.<sup>1</sup>, Trubitsyn M.P.<sup>1</sup>, Volnianskii M.D.<sup>1</sup>,

Volnyanskii D.M.<sup>2</sup>

<sup>1</sup> *Institute for Energy Efficient Technologies and Materials Sciences, Oles Honchar Dnipro National University, prosp. Gagarina, 72, Dnipro, 49010, Ukraine*

<sup>2</sup> *Ukrainian State University of Science and Technologies, vul Lazaryana. 2, 49010 Dnipro, Ukraine*

Lead molybdate crystals ( $\text{PbMoO}_4$ ) are widely known as multifunctional inorganic materials. They are used in acousto-optics, laser technology, and cryogenic scintillation detection systems. Lead molybdate belongs to a large group of crystals with a well-studied structure of the mineral scheelite ( $\text{CaWO}_4$ ). It has a tetragonal structure (space group  $I4_1/a$ ,  $Z = 4$ ). To obtain large crystals, as a rule, the method of pulling from the melt on a seed is used. X-ray diffraction, luminescence, and EPR studies have shown that the crystal lattice of such crystals contains point and extended defects, as well as various clusters, including photoinduced ones, based on anionic  $\text{MoO}_4$  groups that have captured photoelectrons. In fact,  $\text{PbMoO}_4$  single crystals can be considered as a partially disordered medium. This is a characteristic feature of crystals with a scheelite structure.

A preliminary study of the charge transfer mechanism in  $\text{PbMoO}_4$  single crystals showed that hopping conduction occurs in the temperature range up to 700 K. Charge carriers are electrons (holes) moving by activated hops through localized states inside clusters of finite sizes. At higher temperatures, intrinsic or ionic conduction is possible. In the latter case, the conduction is carried out by oxygen ions (oxygen vacancies).

In the present work, we studied the influence of such factors of disordering of the crystal structure as preliminary UV illumination, deviation from the composition stoichiometry, and the choice of crystal modification of the initial components on the charge transfer in  $\text{PbMoO}_4$ . As is known, lead oxide can exist in two polymorphic forms. This is an  $\alpha$ -modification (lead litharge) which has a red color and belongs to the tetragonal syngony (symmetry space group  $P4/nmm$ ,  $Z=4$ ). And  $\beta$ -modification (massicot), the crystals of which are yellow in color and are characterized by rhombic symmetry (space group  $Pbcm$ ,  $Z=2$ ). The study was carried out in the temperature range of 300-700 K.

The results obtained are discussed within the framework of the model of hopping conductivity in disordered media.

# Crystallization of FeBSi metallic glasses annealed in an isothermal and non-isothermal way and characterized by electrical resistivity and absolute thermoelectric power.

K. Khalouk<sup>1</sup>, Y. Plevachuk<sup>2</sup>, I. Kaban<sup>3</sup>, M. Mouas<sup>1</sup>,  
F. Gasser<sup>1</sup> and J.-G. Gasser<sup>1, +</sup>

*1 Université de Lorraine LCP-A2MC*

*2 Ivan Franko National University of Lviv*

*3 Leibniz Institute for Solid State and Materials Research Dresden*

*+ Corresponding author: jean-georges.gasser@univ-lorraine.fr*

Metallic glasses (or amorphous metallic alloys) recrystallize at a given temperature which depends strongly on the heating rate. This behavior is frequently studied by DSC. An alternative and less frequently used method is electronic transport, electrical resistivity and more rarely absolute thermoelectric power (ATP) also called absolute thermopower or absolute Seebeck coefficient. ATP characterizes a material and its measurement, unlike resistivity, does not require knowing the exact geometry of the sample. In addition, X -rays or neutron scattering is used to characterize the structural changes during recrystallization.

The  $\text{Fe}_x\text{B}_y\text{Si}_z$  metallic alloys can be amorphized in a wide range of compositions and the behaviors of obtained metallic glasses (particularly during their recrystallization) depend strongly on the exact composition.

In current work, we present a very precise experimental results on electronic transport of FeBSi metallic glasses measured at a low (compared to the DSC) and constant heating rate, depending on the temperature in the amorphous phase but also once recrystallized. We have also studied the change in electronic transport at a constant temperature of 420 ° C for 34 hours. One can also link the change in electronic transport to the change in the atomic structure factor which, by chance, has been measured. We interpret the results qualitatively within the framework of the extended Faber-Ziman theory, widely studied by some of us, for liquid metallic alloys.



## Peculiarities of tape amorphous alloys surface properties

Hertsyk O.M.<sup>1</sup>, Hula T.H.<sup>1</sup>, Kovbuz M.O.<sup>1</sup>, Yezerska O.A.<sup>2</sup>,  
Kulyk Yu.O.<sup>1</sup>, Pandiak N.L.<sup>3</sup>

<sup>1</sup>*Ivan Franko National University of Lviv, Ukraine*

<sup>2</sup>*Fraunhofer Institut Fertigungstechnik Materialforschung, Germany*

<sup>3</sup>*Ukrainian National Forestry University, Ukraine*

The wide application of amorphous metal alloys (AMA) is based on their unique physicochemical properties, which require additional research according to operating conditions. In the case of tape amorphous metal alloys based on Fe, produced by the method of ultra-fast cooling from the melt, it is also necessary to take into account that the elemental composition and the degree of amorphousness of the surface of the tape, which is directly in contact with the surface of the cooling element, is slightly different from the outer surface. The elemental composition of the AMC tapes surface, determined by the method of X-ray spectral probe microanalysis (Table), differs from the elemental composition of the charge.

Table

The elemental composition of the surface of AMC tapes (at., %)

Elemental composition of the charge							Elemental composition of the surface						
Fe	Ni	Mo	Cu	Nb	Si	B	Fe	Ni	Mo	Cu	Nb	Si	B
78,5	1,0	0,5	-	-	6,0	14,0	91,0	1,1	0,6	-	-	2,1	5,2
73,1	-	-	1,0	3,0	15,5	7,4	78,8	-	-	1,2	2,9	5,4	11,7

Physico-chemical characteristics of amorphous alloys depend on parameters of short-range order and degree of amorphousness. The analysis of the short-range values determined from the scattering intensity curves  $I(s)$  showed that the average interatomic distance  $r_1=0.253$  nm is close to the sum of two atomic radii of Fe ( $R_{Fe}=0.127$  nm), which indicates the predominant influence of microformations  $\alpha$ -Fe in the formation of short-range order. The volume fraction of Fe(Si) crystallites with a size of  $L=1.8$   $\mu$ m indicates the formation of crystallite groups. In the amorphous alloy  $Fe_{73,1}Cu_{1,0}Nb_{3,0}Si_{15,5}B_{7,4}$ , the structural parameters of which are close to those of  $Fe_{78,5}Ni_{1,0}Mo_{0,5}Si_{14,0}B_{6,0}$ , a micro-inhomogeneous phase is observed, the structural elements of which are microregions formed by clusters with short-range order of the type  $Fe_3B$  compounds and microregions rich in Nb atoms. Therefore, the surface of the studied AMA is micro-inhomogeneous, which obviously determines the speed and nature of the surface processes of the alloys.

This work was partly supported by the Simons Foundation (Award Number: 1037973)

# The dependence of electrical and thermoelectric properties of solid solutions $\text{AgSbSe}_2\text{-PbSe}$ on their composition

Novosad O.V.<sup>1</sup>, Shygorin P.P.<sup>1</sup>, Venhryn B.Ya.<sup>2</sup>, Shygorin O.P.<sup>1</sup>

<sup>1</sup>*Lesya Ukrainka Volyn National University, Lutsk, Ukraine*

<sup>2</sup>*Lviv Polytechnic National University, Lviv, Ukraine*

Triple semiconductor compounds of the  $\text{A}^{\text{I}}\text{B}^{\text{V}}\text{C}_2^{\text{VI}}$  type, due to their high thermoelectric quality factor  $ZT$ , are known as materials for thermoelectric generation. For instance, the compound  $\text{AgSbSe}_2$  – is a promising thermoelectric material for high-temperature ranges [1].

In this study, the electrical and thermoelectric properties of monocrystal solid solutions  $\text{AgSbSe}_2\text{-PbSe}$  with 0, 10, 20, 30, 40 mol. %  $\text{PbSe}$  were investigated. The results of similar investigations on monocrystals of  $\text{AgSbSe}_2\text{-PbSe}$  with 92, 95, 100 mol. %  $\text{PbSe}$  are presented in the work [2]. Solid solutions with ~50 – 90 mol. %  $\text{PbSe}$  were found to be two-phase.

It was established that by varying the composition of the  $\text{AgSbSe}_2\text{-PbSe}$ , solid solutions, their electrical and thermoelectric properties can be smoothly adjusted. The investigated compounds exhibited p-type conductivity. The specific electrical conductivity ( $\sigma$ ) of  $\text{AgSbSe}_2\text{-PbSe}$  decreased from  $1.4 \Omega^{-1}\cdot\text{cm}^{-1}$  for  $\text{AgSbSe}_2$  monocrystals (0 mol. %  $\text{PbSe}$ ) to  $10^{-2} \Omega^{-1}\cdot\text{cm}^{-1}$  for  $\text{AgSbSe}_2\text{-PbSe}$  monocrystals with 40 mol. %  $\text{PbSe}$ . Increasing amount of the  $\text{PbSe}$  in  $\text{AgSbSe}_2\text{-PbSe}$  led to an increase in the Seebeck coefficient ( $\alpha$ ) from 530  $\mu\text{V/K}$  to 1100  $\mu\text{V/K}$  for  $\text{AgSbSe}_2$  and monocrystals with a composition of 60%  $\text{AgSbSe}_2\text{-40\% PbSe}$ , respectively. The monocrystals studied in this work, having a high  $\alpha$  value, could be used as materials for sensitive thermosensors.

The thermoelectric power ( $\alpha^2\sigma$ ) of  $\text{AgSbSe}_2\text{-PbSe}$  single crystals ranged from  $49\cdot 10^{-6} \text{ W}/(\text{m}\cdot\text{K}^2)$  for  $\text{AgSbSe}_2$  samples (0 mol. %  $\text{PbSe}$ ) to  $1.1\cdot 10^{-6} \text{ W}/(\text{m}\cdot\text{K}^2)$ .

1. Influence of doping on structural and thermoelectric properties of  $\text{AgSbSe}_2$  / K. Wojciechowski, M. Schmidt, J. Tobola [et al.] // *J. of Electron. Mater.* – 2010. – Vol. 39, No. 9. – P. 2053–2058.
2. Oleksii Novosad, Pavlo Shygorin, Volodymyr Bozhko, Polina Pishova, Bohdan Venhryn, Vasyl Goldun. Electrical and Thermoelectrical Properties of  $\text{PbSe-AgSbSe}_2$  Monocrystals *Proceedings of 16th International Conference on Advanced Trends in Radioelectronics, Telecommunications and Computer Engineering*, Lviv-Slavske, Ukraine, February 22–26, 2022, P. 798–801.

# Structure and mechanical properties of rapidly solidified Zr-Ni-Cr-(Al)-Ag alloys

Shved O.V.

*Ivan Franko National University of Lviv, Ukraine*

One of the most investigated metallic systems characterized by high glass-forming ability and large supercooled liquid region is binary Zr-Ni. The advantages of multicomponent ZrNi-based alloys are not only traditional for amorphous high strength, elasticity and corrosion resistance (with noble metal addition) but furthermore prospects in hydrogen purification and hydrogen storage alloys. The investigation of structural peculiarities of the rapidly quenched quinary and quaternary Zr-based Zr-Ni-Cr-(Al)-Ag alloys with their mechanical properties is presented in this work. Alloys in the form of ribbon (25-30  $\mu\text{m}$ ) were produced by melt spinning (at the cooling rate of  $10^6$  K/s) with the circumferential copper wheel speeds of 18 and 25 m/s. Mechanical properties (hardness and Young's modulus) were measured using nano-indentation method.

Single amorphous phases were obtained as a result of rapid quenching of the  $\text{Zr}_{65}\text{Al}_{7.5}\text{Ni}_{10}\text{Cr}_{10(12.5)}\text{Ag}_{7.5(5)}$  ribbons. Positive influence on the glass forming ability demonstrates the small amounts of Ag addition (5 at. %). An approximant icosahedra phase was established to be formed in quaternary system at compositions  $\text{Zr}_{70}\text{Ni}_{10}\text{Cr}_{12.5}\text{Ag}_{7.5}$  and  $\text{Zr}_{70}\text{Ni}_{10}\text{Cr}_{7.5}\text{Ag}_{12.5}$  ( $a=14.66$  Å). These phases became into an amorphous state only after the rotation speed increased up to 25 m/s. All amorphous ribbons possessed good bending plasticity in contradistinction to the brittleness of those containing additional crystalline phases. The highest hardness and Young's modulus shown alloys consist of nano-size tetragonal  $\beta$ -Zr phase in the amorphous matrix.

# **Modification of the structure of amorphous metal alloys using laser processing methods**

Nykyruy Yu.S., Mudry S.I., Prunitsa V.V.

*Ivan Franko National University of Lviv, Ukraine*

Amorphous metal alloys (AMA) are multi-functional advanced materials, the properties of which are related to a disordering of structure and are very sensitive to structural changes. AMA are metastable materials in which a transition to a more stable state under external influence occurs. A formation of crystalline phases accompanies such a transition and, therefore, changes in the material's properties. The structural transformations in Fe- and Co-based amorphous alloys induced by laser irradiation and associated changes in properties were investigated in present work. The amorphous alloys were synthesized by the melt quenching method in the form of a ribbon 0.025-0.030 mm thick and 10-20 mm wide. For structure modification, we used laser processing methods (laser wavelength of  $1.06\pm 0.01\ \mu\text{m}$  in different modes of laser operation). Focused laser irradiation is capable of causing high-speed heating of the ribbon surface in the local area, resulting in different structural transformations depending on pulse power and duration. Features of structural transformations of irradiated samples were studied by X-ray diffraction method. The obtained results show that the ribbons are partly crystalline after laser treatment. We observed local crystallized regions in amorphous matrices. Based on the X-ray diffraction analysis, the quantitative and qualitative compositions of the formed crystalline phases were determined. Changes in the microstructure of the irradiated surface were studied by scanning electron microscopy, and the microhardness was studied by the Vickers method. The percentage content of the phases in the amorphous matrix and their average grain size depends on time-space features of irradiation. Microscopic studies of the surface indicated that crystallization occurs within the irradiated zone. However, structural transformations associated with the relaxation of the structure and hardened stresses also occur outside of it. Measuring the microhardness of the irradiated areas made it possible to establish a non-linear dependence on the duration of the pulse. The obtained results make it possible to further work on the creation of a spatial configuration with a different degree of structural order in amorphous metals and alloys by laser processing methods.

# Atomic structure and kinetics of phase formation in an amorphous metal alloy $\text{Ni}_{83.7}\text{Fe}_3\text{Cr}_7\text{Si}_{4.5}\text{B}_{2.8}$ during heating.

Kulyk Ju.O., Korolyshyn A.V., Velihovskij A.V.

*Ivan Franko National University of Lviv, Ukraina*

The development of modern technology requires the search and development of new materials that are characterized by a certain complex of mechanical and physicochemical properties. It should be noted that amorphous nickel-based alloys have unique corrosion and electrical properties, which allows them to be used as resistive elements and high-temperature solders. The main problem of obtaining amorphous alloys based on Ni-Si-B is the low tendency of their melts to amorphize during rapid cooling. Solving this problem requires choosing the optimal ratio of the content of metallic (Ni, Fe, Cr...) and metalloid (Si, B...) components. In addition, the effective practical application of these alloys requires a detailed analysis of temperature changes in the atomic structure, electrical and magnetic properties.

In this work, the atomic structure, kinetics, and mechanism of formation of crystalline phases in the amorphous alloy  $\text{Ni}_{83.7}\text{Fe}_3\text{Cr}_7\text{Si}_{4.5}\text{B}_{2.8}$  were studied using the method of high-temperature diffractometry, measuring the temperature dependences of electrical resistance and magnetic susceptibility. Diffraction spectra of the samples were obtained on an automated DRON-3 diffractometer equipped with a UVD-2000 high-temperature vacuum chamber.  $\text{Co}_{K\alpha}$ -radiation monochromatized by reflection from a graphite crystal mounted on a diffracted beam was used. The standard four-probe direct current method was used to measure electrical resistance. The magnetic characteristics of the alloy were studied using a vibrating magnetometer.

As a result of the research, it was established that during heating to  $485^\circ\text{C}$ , a mixture of Ni nanocrystals and a metastable phase (MP) is released from the amorphous phase. Analysis of the crystal structure reveals that MP belongs to the Heisler semiconductor phases with a chemical composition close to  $(\text{Ni,Fe})_2\text{CrSi}$ . When heated to  $575^\circ\text{C}$ , the metastable phase decay, the formation of an ordered solid solution of Ni(Si) and the boride phase  $(\text{Ni,Fe,Cr})_3\text{B}$  is observed. It should be noted that in the temperature range of existence (MP) there is a significant increase in the electrical resistance of the alloy, the probable cause of which is its semiconducting properties. It was established that the specific saturation magnetization of the amorphous  $\text{Ni}_{83.7}\text{Fe}_3\text{Cr}_7\text{Si}_{4.5}\text{B}_{2.8}$  alloy after heating to  $560^\circ\text{C}$ , measured in a magnetic field with an intensity of  $800 \text{ kA}\cdot\text{m}^{-1}$ , is  $\sigma_s = 1.6 \text{ A}\cdot\text{m}^2\cdot\text{kg}^{-1}$ .

## **Phase formation in the amorphous Fe<sub>80</sub>B<sub>20</sub> alloy during heating with alternating electric current.**

S. Mudry, Yu. Kulyk, V. Prunitsa

*Ivan Franko National University of Lviv, Ukraine*

Amorphous iron-based metal alloys are characterised by a unique set of physical, chemical and mechanical properties that depend significantly on the heat treatment methods. The use of the contact electric heating method makes it possible to achieve ultra-high heating rates (400 - 500 °C/s), which leads to a significant shift in phase transitions to the high temperature region. This makes it possible to change the sequence of formation of crystalline phases, which allows the formation of structures with physical and chemical characteristics that cannot be achieved during slow heating.

This work investigates the mechanism and kinetics of phase transformations during the heating of the amorphous Fe<sub>80</sub>B<sub>20</sub> alloy with an alternating electric current of industrial frequency of 50 Hz. The experimental setup included a control transformer (220 V, 50 Hz) and a power transformer. The test specimens were placed in a vacuum chamber with current electrodes connected to the outputs of the secondary winding of the power transformer. The output voltage of the power transformer was varied in the range of 1.1 - 2.1 V. The X-ray analysis of structural transformations was carried out on an automated diffractometer DRON-3 (Cu K $\alpha$  radiation). For comparison, phase transformations in the Fe<sub>80</sub>B<sub>20</sub> alloy were analysed during annealing for 30 min in the temperature range 400-600 °C.

According to the results of the studies of annealed samples, the decomposition of the amorphous phase begins at 400 °C with the release of a solid solution of  $\alpha$ -Fe, the volume fraction of which does not exceed 5%. An increase in the annealing temperature to 425 °C leads to the complete decomposition of the amorphous phase by the eutectic mechanism to form a mixture of metastable Fe<sub>3</sub>B boride (tetragonal syngonium, space group I4/m, lattice parameters  $a \approx 8.60$  Å,  $c \approx 4.30$  Å) and a solid solution of the  $\alpha$ -Fe phase. When the Fe<sub>80</sub>B<sub>20</sub> alloy is heated to 600 °C, the decomposition of metastable boride is observed with the formation of an equilibrium mixture of stable Fe<sub>2</sub>B and  $\alpha$ -Fe boride. At the same time, the sequence of phase transformations changes significantly during AC heating. In the samples treated at voltages in the range of 1.1 - 1.2 V, simultaneous release of Fe<sub>3</sub>B boride (I4/m) and  $\alpha$ -Fe phase is observed. With increasing voltage at the electrodes, a decrease in the proportion of Fe<sub>3</sub>B (I4/m) boride and the appearance of a significant amount of orthorhombic Fe<sub>3</sub>B (Pnma) boride are observed. In addition, the growth of  $\alpha$ -Fe crystallites is oriented in the direction of the crystallographic axis [100

## Секція 4

*Процеси кластеризації та нанокристалізації.*

# Influence of the state of the $C$ atoms on the crystal structure of martensite of carbon steels

V.A. Lobodyuk

*G.V. Kurdyumov Institute for Metal Physics of the N.A.S. of Ukraine*

Concentration of the  $C$  atoms in martensite of carbon steels does not exceed 1.7 wt % ( $\approx 8.2$  at %). It is examined two states of the carbon atoms in martensite of C-steels, disordered and ordered. In the disordered state atoms  $C$  are situated arbitrarily in the three possible of octahedral interstices along directions  $[100]_M$ ,  $[010]_M$  or  $[001]_M$  and in this case corresponding lattice edge increase on the diameter of the  $C$  atom. In the result, the crystal structure of martensite becomes *pseudocubic* in average because the lattice edges are changed differently.

Under ordering, the  $C$  atoms are situated only along directions  $[001]_M$  and in this case the crystal structure of martensite of carbon steels becomes *pseudotetragonal* one.

It is proposed to consider the crystal structure of martensite of carbon steels as system of the lattice blocks. Each block consists of four distorted lattices with  $C$  atom at the common axis of block. In the case of the ordering of  $C$  atoms the block axes directed along  $[001]_M$  only. In the disordered state of the  $C$  atoms, the axes of block may situate along directions  $[100]_M$ ,  $[010]_M$  or  $[001]_M$  arbitrarily.



## Dielectric properties changing at the impurity additions and ageing in selenium-based glasses

Horvat A.A., Molnar O.O., Minkovich V.V., Mikla V.I.

*Uzhhorod National University, Uzhhorod, Ukraine*

Chalcogenide glasses, which can switch repeatedly between solid crystalline and amorphous phases, are of particular interest for example as digital memory, radio frequency switches, reconfigurable meta-optics, tunable emitters and absorbers. This phase change materials (PCM) are attracting attention as promising systems for electronic applications because in doing so their electrical conductivity changes by several orders in magnitude [1,2]. Most chalcogenide glasses based on elementary selenium, for this we investigate stability and influence of small amounts additives of As, Sb, In and Ga on Se-based glasses.

Selenium-based glasses prepared by means of melt quenching technique, amorphous nature of the samples were confirmed by using X-ray diffraction and thermal analysis. The values of the real  $\epsilon'$  and imaginary  $\epsilon''$  components of the complex dielectric constant  $\epsilon^* = \epsilon' + i\epsilon''$  were calculated using a parallel dielectric substitution scheme. The dielectric parameters for the glass samples as a function of temperature at various frequencies in the range 10 Hz – 100 kHz have been studied. From these studies it is clearly conclude that the abovementioned dielectric parameters are solidly affected by replacement of As, Sb, In and Ga additions. Namely, the additions of indium and gallium leads to higher values of dielectric parameters and a sharper crystallization effect, while arsenic and antimony contribute to greater stability of the glassy state.

A similar phenomenon is observed in pure vitreous selenium aged for decades in dark at room temperatures, in which anomalies associated with crystallization observed at much lower temperatures and have a very sharp form in comparison with «fresh» glassy samples.

We believe that In or Ga and structural relaxation at ageing leads to the appearance of additional mechanism of polarization which is probably due to the micro-heterogeneity of the structure and associated with the transition regions between the amorphous matrix and clusters of crystalline phase nuclei. Their presence causes a significant difference in the behavior of dielectric parameters during crystallization of investigated glasses.

1. Golovchak, R., Plummer, J., Kovalskiy, A. *et al.* Phase-change materials based on amorphous equichalcogenides. // Scientific Reports. – 2023. Vol. 13. 2881. <https://doi.org/10.1038/s41598-023-30160-7>.
2. Avik Mandal, Yihao Cui, Liam McRae and Behrad Gholipour. Reconfigurable chalcogenide phase change metamaterials: a material, device, and fabrication perspective. // J. of Physics: Photonics. -2021. - Vol. 3, No 2. 022005. <https://doi.org/10.1088/2515-7647/abe54d>.

## Structural transformations and conductivity of Ni films.

Plyatsko S.V., Gromovyi Yu.S., Dmytruk N.V., Rashkovetskyi L.V.,

Svezhentsova K.

*V.E. Lashkaryov Institute of Semiconductor Physics NAS of Ukraine*

The deposition of the studied Ni films was carried out in a vacuum unit by the magnetron sputtering method. Nickel deposition was carried out from a plate target onto a substrate of sital, single-crystal (100) n-Si with a resistivity of 10 Ohm·cm and a SiO<sub>2</sub> layer with a thickness of 2-5 nm. The sputtering source was a 99.99% pure nickel cathode with a diameter of 40 mm and a thickness of 1.5 mm. A decisive role in the formation of nickel layers is played by the appearance of a wetting layer on the surface of the substrate and the appearance of mismatch stresses, which leads to the formation of 3D clusters on the surface of the Ni buffer layer. The density of 3D clusters increases with increasing film thickness, leading to the formation of 3D cluster domes under controlled growth conditions. The size of the clusters has a large spread in the diameter at the base from 10 to 100 nm. With a further increase in the thickness of the film, the size of the clusters does not change significantly, but at the same time there is a transition to a dense packing of clusters of various shapes (cubic, drop-shaped, elongated, rod-shaped, shapeless and 3D - dome) with clear boundaries between them. The number of 3D-dome clusters in this phase increases slightly. For thicknesses exceeding 150 nm, the morphological structure becomes more smoothed, the clusters merge and appear in the form of hills with no clear boundaries between them. It is quite obvious that each growth phase of the nickel film will correspond to its characteristic conductivity mechanism  $\sigma(h)$ . As the thickness of the films increases, the dependence of  $\sigma(h)$  is characterized by four regions that correspond to different conduction mechanisms. The change in  $\sigma(h)$  occurs at thicknesses of 37 nm, 59 nm, and 150 nm. Extrapolation of the dependence  $\sigma(h)$  to zero thickness gives the value of conductivity  $\sigma = 0$ . The value of the specific conductivity  $\sigma(h)$  for the thickness  $h < 25$  nm is five orders of magnitude smaller than the bulk conductivity for nickel ( $\sigma_{Ni} = 8.5 \cdot 10^4 \text{ Ohm}^{-1} \text{ cm}^{-1}$ ). In addition, there is a certain critical metal content  $x = x_c$  (flow threshold), below which the conductivity is determined by electron tunneling between individual nanostructures, which is a sign of hopping conductivity. Apparently, all the listed mechanisms contribute to the conductivity behavior at small film thicknesses. As the thickness of the film increases, when the regions of the nanoclusters overlap (percolation phenomenon), the conductivity increases dramatically. When a thickness of 150 nm is reached, the nanoclusters merge and the conductivity becomes close to the bulk conductivity, the dependence of  $\sigma(h)$  is weakly expressed.

## **Clusterization in solutions as a process of mesophase formation**

Bulavin L.A., Zabashta Yu.F., Lazarenko M.M., Vergun L.Yu., Alekseev A.N.,  
Kovalchuk V.I., Brytan A.V.

*Taras Shevchenko National University of Kyiv,  
Faculty of Physics, Department of Molecular Physics, Ukraine*

The thesis about existence of clusters in solutions is generally accepted (see, for example, [1]). The question of the physical mechanism causing the appearance of these clusters remains debatable.

The clustering in solutions can be considered as a phase transition of the first kind is shown in this report. The result of this phase transition is the formation of a mesophase that is an intermediate between the solution and the crystalline phase. Unlike the solution in the mesophase, the particles of the dissolved substance, connecting with each other, form a framework.

The thermodynamic conditions of mesophase formation were analyzed. It is shown that a main role in this process is played by the occurrence of oscillatory modes. These modes associated with the appearance of the framework. The general appearance of the phase diagram is defined, which assumes the existence of three phases in the "solvent - solute" system, namely, solution, crystalline phase, and mesophase.

The reality of the existence in solutions the first order phase transitions, which are accompanied by the formation of a mesophase, was verified experimentally. The objects of the study were representatives of two classes of solutions: low-molecular (aqueous solutions of glucose) and high-molecular (aqueous solutions of cellulose derivatives). The light scattering in these solutions was studied in the temperature range of 20-80°C. It was found that at certain temperatures, fluctuations in the intensity of scattered light reach their maximum value, which is typical (see, e.g., [2], etc.) for the temperatures of the first order phase transition. The mentioned temperatures are identified with the temperature of the "solution-mesophase" phase transition.

1. L.A.Bulavin Y.F.Zabashta, L.Yu.Vergun, K.O.Ogorodnik. Saccharide solutions under the magnetic field action// Ukr. J. Phys..-2016.- №7, V. 61.- P. 589-593.
2. L.A. Bulavin, Yu.F. Zabashta, M.M. Lazarenko, L.Yu. Vergun, K.O. Ogorodnik, K.I. Hnatiuk. Autowaves induced by first-order phase transitions. Ukr. J. Phys.- 2022. Vol. 67, No. 4.- P.270-276.

# Energy band gap and optical properties of CdTe spherical quantum dots calculated by DFT

Deva L.R.<sup>1</sup>, Semkiv I.V.<sup>1</sup>, Kashuba A.I.<sup>1</sup>, Petrus R.Y.<sup>2</sup>

<sup>1</sup>*Lviv Polytechnic National University, Bandera Str. 12, 79646 Lviv, Ukraine*

<sup>2</sup>*Carl von Ossietzky University of Oldenburg, Institute of Physics, Carl-von-Ossietzky-Straße 11, 26129 Oldenburg, Germany*

Nanocrystalline semiconductor materials of II–VI group offer unique electronic and optical properties attributed to the so-called quantum confinement effects [1]. The optical properties of such compounds can be adjusted by altering the dimensions of the nanoparticles. CdTe quantum dots (QDs), is an important II–VI group semiconductor material with a narrow bulk band gap (~1.5 eV) and a high excitation Bohr radius (7.3 nm) [1, 2]. QDs based on CdTe have potential applications in novel light emitters, next-generation solar cells, sensing, and biomedical diagnostics [3].

CdTe spherical QDs with changing radius ( $R$ ) between 0.5 and 10 nm are studied. These CdTe QDs have zinc-blende symmetry. All calculations including geometry optimization, energy spectra, density of states and optical properties of the CdTe spherical QDs were made using density functional theory (DFT). Density functional GGA+PBE was used to describe the exchange–correlation energy of the electronic subsystem with Hubbard corrections (GGA+ $U$ ). To accurately describe the electronic spectrum, two Hubbard corrections were selected the studied objects: for  $d$ -orbitals Cd ( $U_{4d}$ = 5.80 eV) and  $p$ -orbitals Te ( $U_{5p}$ = 2.55 eV).

The quantum confinement was obtained to have a major effect on the value of the energy band gap and optical properties of CdTe spherical QDs. The energy band gap increases as radius ( $R$ ) of the CdTe spherical QDs decreases. The maximum value of the energy band gap was obtained for CdTe spherical QDs with  $R$ = 0.5 nm ( $E_g$ = 1.418 eV for bulk CdTe). This value is very good correlated with the experimentally obtained in Ref. [4] (~2.3 eV for  $R$ = 2 nm).

1. M. Akbari, et al., CdTe quantum dots prepared using herbal species and microorganisms and their anti-cancer, drug delivery and antibacterial applications// *Ceramics International*. –2020. – Vol. 46. –P. 9979-9989.
2. Y.-J. Yang, et al., Fluorescent mesoporous silica nanotubes incorporating CdS quantum dots for controlled release of ibuprofen// *Acta biomaterialia*. –2009. – Vol. 5. –P. 3488-3496.
3. V. Dzhagan, et al., Tuning the photoluminescence of CdTe quantum dots by controllable coupling to plasmonic Au nanoparticles// *Physics and Chemistry of Solid State*. –2022. – Vol. 23. –P. 720-727.
4. Y. Mastai, G. Hodes, Size quantization in electrodeposited CdTe nanocrystalline films// *J. Phys. Chem. B*. –1997. – Vol. 101. –P. 2685-2690.

## Structural transformations and optical properties of silicon oxide films doped with tin

Voitovych V.V<sup>1</sup>, Rudenko R.M<sup>1</sup>, Poroshin V.M<sup>1</sup>, Kras'ko M.M<sup>1</sup>,

Kolosiuk A.G<sup>1</sup>, Povarchuk V.Y<sup>1</sup>, Voitovych M.V<sup>2</sup>

<sup>1</sup>*Institute of Physics, National Academy of Sciences of Ukraine*

<sup>2</sup>*Laskarev Institute of Semiconductor Physics, National Academy of Sciences of Ukraine*

There are many methods of forming nano-sized crystalline silicon (nc-Si), among which methods based on the use of metals should be highlighted [1,2]. It is known that the crystallization temperature of amorphous silicon can be significantly lowered with the help of metal impurities. The purpose of this work was to study the influence of tin on the surface morphology and structural features of silicon oxide films. Also, to investigate the optical properties of such structures.

Research was conducted on samples of thin-film silicon oxide material doped with tin (nc-Si/SiO<sub>2</sub>/Sn). The samples were obtained as a result of thermal evaporation in a vacuum ( $\sim 10^{-3}$  Pa) from a tantalum ring of a mixture of powders of SiO (Cerac Inc. purity 99.9%) and Sn (grain size 40-45  $\mu\text{m}$ ), taken in different weight percentages (10 %-Sn, 90%-SiO). Heating of the tantalum trough was carried out by the resistive method. Film deposition took place on silicon and sapphire substrates.

It was established that spherical tin-silicon clusters are formed in the oxide matrix at a tin concentration of 2.5 at. % and more. Agglomerations can increase in volume as a result of the union of their own kind. At high concentrations of tin, clusters can be commensurate or even larger than the thickness of the film itself.

From the obtained results, it can be concluded that for nc-Si/SiO<sub>2</sub>/Sn samples, the ultimate solubility of tin atoms is  $\sim 2.5$  at. %, if the concentration of Sn is greater than the limit, then silicon-tin clusters are observed in the films. It is shown that the presence of tin admixture in silicon oxide films does not affect the processes of its transformation from SiO<sub>x</sub> ( $x \approx 1.1$ ) to SiO<sub>2</sub>.

The presence of tin in the silicon-oxide matrix leads to a shift of the maximum PL intensity of the samples to the short-wavelength region of the spectrum and a significant increase in the emissivity of the samples, which significantly expands the possibilities of using this material in optoelectronics.

1. Toyohiko J. Konno, Robert Sinclair. Crystallization of silicon in aluminium/amorphous-silicon multilayers. *Philosophical Magazine Part B*. 1992. Vol. 66, Iss. 6. P. 749.
2. Jeon M., Jeong C., Kamisako K. Tin induced crystallisation of hydrogenated amorphous silicon thin films. *Materials Science and Technology*. 2010. Vol. 26, Iss. 7. P. 875.

# Nanostructuring of the monocrystalline silicon surface under the action of laser pulses

Mohylyak I.A.

*Pidstryhach Institute for Applied Problems of Mechanics and Mathematics,*

*Naukova Str. 3B, 79060, Lviv, Ukraine*

[mohylyak@gmail.com](mailto:mohylyak@gmail.com)

Over the past decade, nonlinear interactions between powerful laser pulses and materials have opened great opportunities in the field of laser micro-nanostructuring [1].

The possibility of micro-nanostructuring of monocrystalline silicon has been experimentally investigated using two types of lasers – pulsed ruby laser GOR-300 type ( $\lambda = 0,69 \mu\text{m}$ ,  $\tau_i = 5 \text{ ms}$ ), pulsed YAG:Nd<sup>3+</sup> laser LTY-205-1 type ( $\lambda = 1,06 \mu\text{m}$ ), which operated in mode of the modulated Q factor ( $\tau_i = 15 \text{ ns}$ ,  $E = 0.1 - 0.4 \text{ J/cm}^2$ ) or free generation ( $\tau_i = 1 \text{ ms}$ ,  $E_{\text{max}} = 30 \text{ J/cm}^2$ ). It is shown that the melting of Si at threshold values of the energy of laser radiation has a local character and the shape of crystallized melts depends on the crystallographic orientation of the samples.

The results of microscopic investigations by electron microscope of periodic structures formed on the Si surfaces with crystallographic orientation (111), (100) are presented. Different types of periodic structures were obtained, such as micropyramids with square and triangular bases. Previous studies have interpreted that the LIPSS is formed by the interference between the incident laser field and the surface electromagnetic wave formed at the rough surface such as surface plasmon polaritons. Thus, the structural shape of the LIPSS can be easily manipulated by changing the optical parameters, such as polarization, incident angle, and input wavelengths [2]. Surface periodic structures with nanometer dimensions range are obtained. That can be used to create effective photovoltaic converters of solar energy. The obtained results extend the idea of nonequilibrium melting and crystallization processes of semiconductors and can be used for controlled surface structuring for the purposes of micro-nanoelectronics.

1. Ye.F. Venger, O.Yu. Semchuk, O.O. Havrylyuk. Lazer-indukovani nanostruktury v tverdykh tilakh. – K.: Akadempriodyka, 2016. – 236 p.
2. I.A. Mohylyak, O.Yu. Bonchyk, S.A. Korniy, S.G. Kiyak, D.I. Popovych. Laser formation of periodic micro- and nanostructures on the surface of monocrystalline silicon // Physics and chemistry of solid state. – 2020. – V.21, No 2. – pp 215-218.

# Laser-induced transformations in thermally evaporated thin TlInSe<sub>2</sub> films studied by Raman spectroscopy

Azhniuk Y. M.<sup>1</sup>, Gomonnai A. V.<sup>1,2</sup>, Lopushansky V. V.<sup>1</sup>,  
Gomonnai O. O.<sup>2</sup>, Babuka T.<sup>2</sup>, Loya V. Y.<sup>1</sup>, Voynarovych I. M.<sup>1</sup>

<sup>1</sup> *Institute of Electron Physics, Nat. Acad. Sci. Ukr., Uzhhorod, Ukraine*

<sup>2</sup> *Uzhhorod National University. Uzhhorod, Ukraine*

TlInSe<sub>2</sub> is a known semiconductor material with chain-like structure, promising for applications in optoelectronics. In the recent years an additional research interest towards thin TlInSe<sub>2</sub> films emerged [1]. Here we present a Raman spectroscopic study of structural transformations in thermally evaporated thin TlInSe<sub>2</sub> films under illumination by a tightly focused laser beam.

TlInSe<sub>2</sub> films with thickness  $d$  from 10 to 200 nm were prepared by thermal evaporation on cold silicon and silicate glass substrates. Micro-Raman scattering measurements were carried out at room temperature using an XPloRa Plus spectrometer (Horiba). Excitation was provided by a 532 nm solid-state laser. The scattered light was detected by a cooled CCD camera. The instrumental resolution was better than 2.5 cm<sup>-1</sup>.

Features in the Raman spectra of the films measured at a low excitation power density  $P_{\text{exc}}=4$  kW/cm<sup>2</sup> are noticeably broader than for single-crystal TlInSe<sub>2</sub> which can be an evidence of the amorphous structure of the films. In our case the spectral position of the main maximum is closer to 165 cm<sup>-1</sup> rather than 183 cm<sup>-1</sup> as expected for TlInSe<sub>2</sub> and observed for polycrystalline films prepared on heated substrates [1]. This is explained by the difference in the preparation conditions which in our case lead to the formation of amorphous films..

With  $P_{\text{exc}}$  increasing to 40 kW/cm<sup>2</sup> the Raman spectra of the TlInSe<sub>2</sub> films reveal intense narrow maxima which clearly indicates fast crystallization of the film material in the laser spot. However, besides a sharp peak near 182 cm<sup>-1</sup> which is the most intense known Raman feature of TlInSe<sub>2</sub>, a narrow peak near 160 cm<sup>-1</sup> is also revealed. The latter is known to be the most prominent Raman feature of crystalline TlSe. This fact indicates that upon intense illumination by a tightly focused laser beam with above-bandgap energy two types of crystallites (TlInSe<sub>2</sub> and TlSe) are formed on the surface of the TlInSe<sub>2</sub> amorphous films. This crystallisation effect is local (within the laser spot) and irreversible. The effect is driven by a thermal mechanism when the sample surface is heated by the tightly focused laser beam and thermally enhanced diffusion enables the crystallite formation.

1. Al-Harbi F. F., Darwish A. A. A., Hamdalla T. A., Abd El-Rahman K.F. Structural analysis, dielectric relaxation, and AC electrical conductivity in TlInSe<sub>2</sub> thin films as a function of temperature and frequency // Appl. Phys. A. – 2022. – Vol. 128. – P. 622 (9 pp).

# Structure and Electrical Properties of $\beta$ -Ga<sub>2</sub>O<sub>3</sub> Films Obtained by Radio Frequency Magnetron Sputtering on template Si/porousSi/Si

V. V. Kidalov,<sup>1</sup> A. F. Dyadenchuk,<sup>1</sup> M. P. Derhachov,<sup>2</sup>

<sup>1</sup> *Dmytro Motornyi Tavria State Agrotechnological University, Ukraine*

<sup>2</sup> *Oles Honchar Dnipro National University, Dnipro 49010, Ukraine*

$\beta$ -Ga<sub>2</sub>O<sub>3</sub> films are widely applied in gas sensors, phosphors, lithium batteries, and antireflection coatings in solar cells.

By now  $\beta$ -Ga<sub>2</sub>O<sub>3</sub> films have been successfully obtained by techniques such as molecular beam epitaxy, chemical vapor deposition of organometallic compounds, ultrasonic pyrolytic sputtering, radio frequency sputtering, chloride-based vapor epitaxy, and others.

We obtained polycrystalline Ga<sub>2</sub>O<sub>3</sub> films on nanoporous silicon using the RF magnetron sputtering technique [1]. The nanoporous layer overcomes the problem of mismatch between the Ga<sub>2</sub>O<sub>3</sub> and Si lattices, but during the growth of the Ga<sub>2</sub>O<sub>3</sub> film in an oxygen atmosphere, the silicon surface will be covered with a layer of amorphous SiO<sub>2</sub>, as was shown by us [1], on which the epitaxial Ga<sub>2</sub>O<sub>3</sub> film will not grow, but only the polycrystalline Ga<sub>2</sub>O<sub>3</sub> film will grow.

In this message, we consider the possibility of obtaining an epitaxial Ga<sub>2</sub>O<sub>3</sub> film on a SiC/porous Si/Si template by the method of magnetron sputtering. At the same time, the intermediate nanoporous layer will relieve mechanical stresses due to the mismatch between the Si and SiC lattices. And the SiC film will protect the silicon from the interaction with oxygen during the growth of the Ga<sub>2</sub>O<sub>3</sub> film by magnetron sputtering.

Characterization of the samples, using such tools as scanning electron microscopy (SEM), energy dispersive X-ray spectroscopy (EDAX), X-ray diffraction (XRD), Raman spectroscopy and impedance spectroscopy.

The research was supported by the Ministry of Education and Science of Ukraine, namely: STW No. 0121U109519.

1 V.V.Kidalov, A.F.Dyadenchuk, V.P.Kladko, O.I.Gudymenko, M. P. Derhachov, S. O. Popov, O. O. Sushko, Vitali V.Kidalov. Structure and electrical properties of  $\beta$ -Ga<sub>2</sub>O<sub>3</sub> films obtained by radio frequency magnetron sputtering on porous silicon /ECS Journal of Solid State Science and Technology. - 2022. -Vol. 11 (2). - P. 025004.



## Секція 5

*Фізичні явища в нанокмпозитних системах.*

# **Magnetocapacitance Effect in Tunnel Contact with Perpendicular Anisotropy of Magnetic Electrodes**

Konoplyuk S.M., Krupa M.M.

*Institute of magnetism of NASU and MESU, Kyiv, Ukraine*

In this report, we want to consider the features of the magnetocapacitive effect in tunnel magnetic contacts with perpendicular magnetization of magnetic electrodes. Great interest in magnetic tunnel junctions is caused by the fact that not only a large value of tunnel magnetoresistance is obtained in them, but also by the fact that in recent years in tunnel contacts with interfaces of the Fe/MgO type, a significant change in the capacitance in the magnetic field has been experimentally registered, which is associated from the appearance of spin capacitance at the magnetic metal/dielectric interface. This effect is called the magnetic tunneling capacity (MTC) effect, and it is considered one of the most promising effects that may have practical applications in memory cells and other spintronic devices. In contact tunnels with perpendicular anisotropy, the antiparallel orientation of magnetization radically changes the distribution of the magnetic field in the contact barrier layer and causes the appearance of a high-gradient magnetic field in the direction of magnetization of the contact magnetic electrodes. Under the action of such a high-gradient field, there is a spatial separation of spin-polarized major and minor electrons of electrons in the interface region, which creates an inhomogeneous distribution of electric charge in the contact barrier layer. As a result, an additional energy barrier for major spin-polarized electrons appears near each of the magnetic electrodes, and an additional effective capacitance, called spin capacitance, appears in the contact barrier layer. This additional spin capacitance can significantly reduce the total capacitance of the tunnel magnetic contact. The value of such additional spin capacity is proportional to the value of the spin polarization of electrons in the magnetic electrodes and the value of the magnetic field gradient with antiparallel orientation of their magnetizations. The mechanism of tunnel magnetic capacitance described by us is not only fundamentally different from the mechanism of tunnel magnetic capacitance in tunnel contacts with Fe/MgO interface boundaries, but also, in our opinion, has a better prospect for practical use. The large values of TMR and TMC in tunnel contacts with Fe/MgO interfaces are related to the features of the electronic structure of the Fe/MgO interface, where the effective spin-dependent tunneling effect is ensured by a good agreement between the crystal lattice parameters of the iron magnetic electrode and the crystal lattice parameters of the magnesium oxide nanolayer. In tunnel magnetic contacts with perpendicular magnetization of the electrodes, such matching of the grid of the magnetic electrode and the barrier nanolayer is not a strict necessity, which allows to simplify their manufacturing technologies. We conducted experimental studies of magnetoresistance and magnetocapacitive effect in tunnel magnetic contacts Tb 22 Co 5 Fe 73 /Pr 6 O 11 /Tb 19 Co 5 Fe 76 with perpendicular magnetization of magnetic electrodes and a paramagnetic barrier layer. At room temperature, the value of tunnel magnetic resistance exceeds 110%, and the value of tunnel magnetic capacitance exceeds 115%.

## Some features of preparation 2D functional materials

Bohdan Tsizh<sup>1,2</sup>, Stepan Mudry<sup>3</sup>

<sup>1</sup>*Kazimierz Wielki University in Bydgoszcz, Poland*

<sup>2</sup>*Stepan Gzytskyi National University of Veterinary Medicine and Biotechnologies Lviv, Ukraine*

<sup>3</sup>*Ivan Franko National University of Lviv, Ukraine*

2D thin film materials are a special group of modern materials that is constantly expanding. In connection with the growing use of smart materials and devices, the preparation of thin-film materials with a predetermined complex of their physical and technical properties is becoming more and more relevant.

To date, dozens of various ways of obtaining thin-film materials have been deeply studied and worked out, their classification has been carried out, and detailed recommendations have been developed for specific materials and purposes [1]. However, taking into account the complexity and precision of the known technological processes, the issues of choosing a method of obtaining thin-film materials and structures, their nanostructuring, alloying and processing, as well as choosing the optimal technological parameters of the synthesis, remain relevant.

In recent decades, organic materials are increasingly used in all spheres of human activity. In this report, on the basis of studies of optical absorption spectra of films of polyacenes - anthracene, tetracene, tetrachlorotetracene, pentacene and tetrathiotetracene, as well as films of phthalocyanines - H<sub>2</sub>Pc, Cu<sub>2</sub>Pc, ClAlClPc, PbPc, it is experimentally confirmed that the planar structure of atoms of molecular crystals, and therefore the number of  $\pi$ - of electrons responsible for exciton absorption in the visible region of the spectrum determines the position of the edge of their own optical absorption. It was also confirmed that the long-wavelength shift of the optical absorption edge of thin films of phthalocyanines is observed when atoms of heavy elements, for example, lead, are introduced into the molecule. An explanation of such changes is presented based on the interaction of foreign atoms with the  $\pi$ -electron system of phthalocyanine rings of neighboring molecules.

The significant influence of technological parameters of production, in particular, substrate temperature during thermal sputtering, on the crystal structure and optical properties of thin films of linear polyacenes and metallophthalocyanines has been demonstrated and substantiated. The possibility of controlling and presetting the necessary properties of thin-film condensates of molecular crystals is shown.

1. Frey Hartmut, & Khan Hamid R. (2015). Handbook of Thin Film Technology, Springer.

# Synthesis of ZnO photocatalyst

Klimenkov O.M., Ivanenko I.M.

*National Technical University of Ukraine  
"Igor Sikorsky Kyiv Polytechnic Institute", Ukraine*

The problem of water pollution mostly arises due to the high content of pollutants in wastewater coming from households, enterprises, agriculture, and solid domestic and industrial waste landfills. Enterprises produce a large amount of chemically harmful and toxic pollutants, which eventually poison the water. One of these enterprises is the textile industry, which is responsible for the discharge of effluents into rivers, lakes, reservoirs, etc. Such effluents usually contain metals, salts, and various dyes, which have a harmful effect not only on the flora and fauna with which these pollutants have direct contact but also on humans, primarily due to their carcinogenic nature and general toxicity.

To date, many studies are being conducted to improve the efficiency of existing water treatment methods and reduce the economic costs of their operation. Among them are ion exchange, ultrafiltration, flocculation, adsorption, reverse osmosis, and photocatalysis. Photocatalysis is especially desirable for the treatment of polluted wastewater from textile, paper-cardboard, and leather industries, as it allows direct oxidation of dye molecules to the simplest compounds ( $N_2$ ,  $H_2O$ , and  $CO_2$ ) and during the entire process, no toxic pollutants are released as by-products. Moreover, this technique is environmentally safe and has easily controlled parameters [1].

Semiconducting metal oxides are typical representatives of heterogeneous photocatalysis, due to their adjustable structure they are able to mineralize various organic compounds and are inexpensive. One of them is zinc oxide (ZnO) is a low-cost, photosensitive, widespread, and non-toxic photocatalyst that adsorbs a photon from ultraviolet radiation, thereby generating superoxide anion ( $O_2^-$ ) and hydroxyl radical ( $OH^\bullet$ ). ZnO is an n-type conductor with a relatively wide band gap, but despite this, it is a promising candidate for successful use in further research on photocatalysis [1].

The synthesis of ZnO can be carried out by thermal decomposition, electrodeposition, hydrothermal method, organometallic chemical vapor deposition, ultrafast microwave method, pulsed laser deposition, molecular beam epitaxy, etc. Most of these methods require high energy consumption as well as operational costs. Also, most of them have low product yields. The most promising method of ZnO synthesis is the sol-gel method, which allows for obtaining particles with dimensional uniformity and controlled morphology. Also, the synthesis process itself is carried out without using excessive temperatures, it is stable and universal [1].

1. Hutsul K., Ivanenko I., Krymets G. The precipitation synthesis of zinc (II) oxide for photocatalytic degradation of anionic and cationic dyes // Applied Nanoscience. – 2021. – 12 (3). – P. 755-759.

## The effect of 1 MeV electron irradiation on the array of graphene quantum dots in reduced graphene oxide in a wide temperature range of 4.2–300 K

Rudenko R.M.<sup>1</sup>, Voitsihovska O.O.<sup>1</sup>, Abakumov A.A.<sup>2</sup>, Bychko I.B.<sup>2</sup>,  
Poroshin V.N.<sup>1</sup>

<sup>1</sup> *Institute of Physics, National Academy of Sciences, Kyiv 03680, Ukraine*

<sup>2</sup> *L.V. Pisarzhevskii Institute of Physical Chemistry, National Academy of Sciences, Kyiv, 03028, Ukraine*

e-mail: rudenko.romann@gmail.com

This research is aimed the study the effect of 1 MeV electron irradiation on the quantum-dot-like electrical conductivity of an array of graphene quantum dots (GQDs) located in a reduced graphene oxide (RGO). The electrical properties were analyzed in a wide temperature range of 4.2–340 K for doses of 0–160x10<sup>15</sup> cm<sup>-2</sup>. The localization length, dielectric permittivity, and density of localized states were estimated. It was found that the conductivity and charge localization parameters exhibit non-monotonic behavior depending on the irradiation dose. It can change several times in the vicinity of a dose of 10x10<sup>15</sup> cm<sup>-2</sup> compared to the higher or lower dose. It is shown that electron irradiation affects the disordered surrounding matrix, which leads to an increase in the content of oxygen and functional groups. At the same time, the size of the *sp*<sup>2</sup>-carbon domains does not depend on the irradiation dose. It is assumed that electron irradiation indirectly affects the properties of GQDs. The transformation of the surrounding disordered matrix leads to a modification of the electronic properties of the GQDs array and the RGO as a whole. The non-monotonic behavior of the RGO conductivity upon irradiation is due to the features of the energy spectrum of the GQDs array, which is characterized by the presence of periodic peaks in the density of states. The irradiation-induced structural modification likely leads to a shift in the Fermi level and a change in the density of states. At temperatures above 310 K, the RGO conductivity exhibits an Arrhenius behavior with an activation energy of about 60 meV due to charge carrier delocalization at thermal excitation into the extended band.

1. O.O. Voitsihovska, et al. The effect of electron irradiation on the electrical properties of reduced graphene oxide paper, *Mater. Lett.* 236 (2019) 334.
2. R. Rudenko, et al. Dielectric and electrical properties of reduced graphene oxide paper after electron irradiation, *Low Temp. Phys.* 48 (2022) 832.
3. O.O. Voitsihovska, et al. Quantum-dot-like electrical transport of free-standing reduced graphene oxide paper at liquid helium temperatures, *Diam.Relat. Mater.* 130 (2022) 109538.

# Collective Leggett mode in disordered two-phase superconducting ceramics

Shamaev V.V.<sup>1</sup>, Boliasova O.O.<sup>2</sup>, Tarenkov V.Yu.<sup>2</sup>, Shapovalov A.P.<sup>2</sup>

<sup>1</sup>Donetsk National Technical University, Pokrovsk, Ukraine

<sup>2</sup>Kyiv Academic University, Kyiv, Ukraine

Half a century ago, Leggett predicted the existence of a charge neutral and gapped mode in multiband and/or multiphase superconductors. For multiple Josephson-coupled media, the Leggett mode corresponds to collective excitations of the relative phase of different superconducting nanoparticles, which are similar to the plasma mode in multiterminal Josephson junctions and strongly depend on the pairing symmetry as well as the interplay between intra- and intergrain Josephson strengths.

The studied high- $T_c$  Bi-Sr-Ca-Cu-O system is known by strong structural disorder at microscopic and mesoscopic levels. Our samples exhibiting zero resistance were prepared by usual solid-state reaction using powder reagents of  $\text{Bi}_2\text{O}_3$ ,  $\text{SrCO}_3$ ,  $\text{CaCO}_3$ , and  $\text{CuO}$ . They showed two stepwise transitions in the electrical resistance versus temperature curves with onset temperatures of 114 K and 80 K, suggesting coexistence of two phases with different critical temperatures  $T_c$ . Their emergence is explained as the result of the formation of topological defects in a system driven through a continuous phase transition at a finite rate. By bringing a sharp Ag tip in contact with the surface of a superconducting ceramics, we created ballistic contact whose differential conductance  $G(V) = dI(V)/dV$  as a function of the voltage bias  $V$  provides valuable insight on the gap values, its symmetry and the presence of collective excitations in the system.

The conductance spectra  $G(V)$  have consistently demonstrated the presence of multiple peaks outside the gap region, which gradually disappeared with increasing temperature and/or magnetic fields up to critical values  $T_c$  and  $H_{c2}$ , thus proving their relation to superconductivity. Following the Leggett idea, we can attribute the features to elastic charge scatterings by a collective mode inherent in the superconducting state. The peak positions were found to be multiples of the voltage  $\delta \approx 9.8$  mV and satisfying the expected relation  $\Omega_n = n\delta$  for  $n = 3, 4, 5$ , and  $6$ . The absence of visible harmonics corresponding to integer values  $n = 1$  and  $2$  can be explained by the significant steepness of the conductance spectrum part where the features are expected. We believe that their study in other superconducting compounds will contribute to further understanding of the physics of collective excitations in disordered super fluids.

This work was partly supported by the National Research Foundation of Ukraine through the project 2020.02/0408 and the National Academy of Sciences of Ukraine through the research project No. 0121U110080 (Kyiv Academic University).

# Synthesis and band gap of ZnO/TiO<sub>2</sub> nanocomposites

Hutsul Kh.R., Ivanenko I.M.

*National Technical University of Ukraine "Igor Sikorsky Kyiv Polytechnic Institute"*

Semiconductor nanostructures have attracted considerable attention of researchers in recent years due to their unique properties. Some electronic, optical, and catalytic properties are observed only for nanoscale structures. Zinc oxide (ZnO) is a well-known semiconductor with a wide bandgap in the near ultraviolet  $\sim 3.37$  eV at room temperature. High exciton binding energy in ZnO ( $\sim 60$  meV) is much larger than in other semiconductor materials such as ZnSe (22 meV) and GaN (22 meV). ZnO has been investigated over the past decade due to its interesting optical and electrical properties [1-3].

One of the simplest but effective methods of obtaining nanostructured ZnO is the deposition method. In the presented work, the synthesis of the ZnO/TiO<sub>2</sub> composite photocatalyst was carried out by the method of precipitation of intermediate hydroxides and their hydrolysis on the surface of the TiO<sub>2</sub> powder of Evonik P25 (to obtain three different mass ratios of ZnO to TiO<sub>2</sub>). The synthesis scheme is shown in Fig. 1.

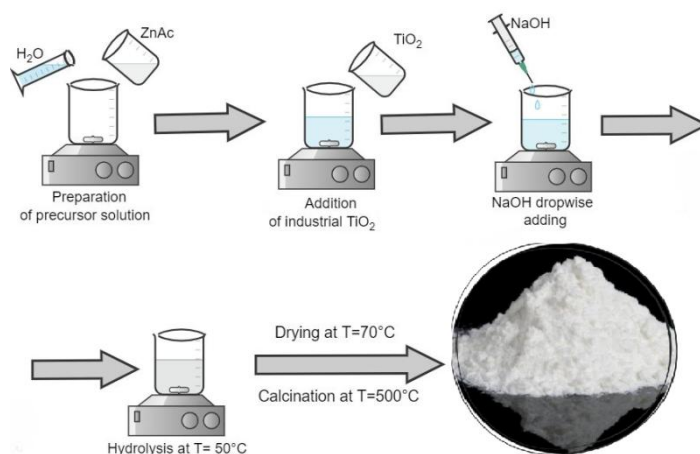


Fig. 1 – Synthesis scheme of ZnO/TiO<sub>2</sub> composite by deposition method

To determine the optical band gap, the absorption spectra of the obtained samples of the ZnO/TiO<sub>2</sub> composite photocatalyst in distilled water were recorded. For this, 1 mg of photocatalyst powder was mixed with 4 mL of distilled water and treated with ultrasound to obtain a homogeneous colloidal suspension, after which the absorption spectrum of the resulting suspension was recorded.

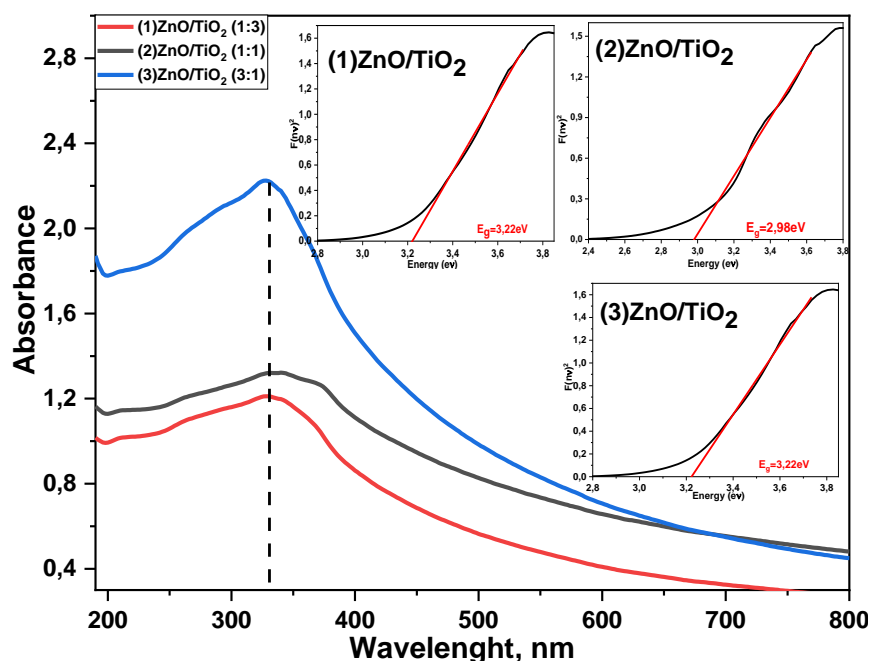


Fig. 2 – Absorption spectra and Kubelka-Munk diagrams of synthesized composites (1)ZnO/TiO<sub>2</sub>; (2)ZnO/TiO<sub>2</sub> and (3)ZnO/TiO<sub>2</sub>.

The obtained measurement results are presented in Fig. 2. The absorption spectra show that the  $\lambda_{\max}$  of all three composites is approximately within the same limits and is  $\sim 335$  nm, and the absorption intensity increases with increasing ZnO content.

The optical band gap was determined using the Kubelka-Munk algorithm [2,3]. As we can see from the obtained results, the value of the optical band gap ( $E_g$ ) for the (1)ZnO/TiO<sub>2</sub> and (3)ZnO/TiO<sub>2</sub> composites is 3,22 eV, and for the (2)ZnO/TiO<sub>2</sub> is 2,99 eV. This means that the composite (2)ZnO/TiO<sub>2</sub> has an optimal band gap to absorb visible light and minimize photogenerated electron-hole recombination, which will contribute to its high photocatalytic activity.

1. H.She, X.Ma, K.Chen, H.Liu, J.Huang, L.Wang, Q.Wang Photocatalytic H<sub>2</sub> production activity of TiO<sub>2</sub> modified by inexpensive Cu(OH)<sub>2</sub> co-catalyst // J. Alloys Compd. – 2020. – Vol.821.
2. I.Ivanenko, K.Hutsul, G.Krymets The precipitation synthesis of zinc (II) oxide for photocatalytic degradation of anionic and cationic dyes // Applied Nanoscience. – 2021. – Vol.11. – P.1-5.
3. I.Ivanenko, K.Hutsul, Y.Fedenko Nanocomposite TiO<sub>2</sub>-ZnO for Dyes Photocatalytic Degradation // 2021 IEEE 11th International Conference Nanomaterials: Applications & Properties (NAP). – 2021. – P.1-4.



# Phase transition at critical bending of a magneto-active elastomer beam

Kalita V. M.<sup>1,2,3</sup>, Dzhezherya Yu. I.<sup>1,2</sup>, Cherepov S. V.<sup>2</sup>, Skirta Yu. B.<sup>2</sup>,  
Bodnaruk A. V.<sup>1</sup>, Ryabchenko S. M.<sup>1</sup>

<sup>1</sup> *Institute of Physics, NAS of Ukraine, Prospekt Nauky 46, Kyiv 03028, Ukraine*

<sup>2</sup> *Institute of Magnetism of the NAS of Ukraine and MES of Ukraine, 36-b Vernadsky Blvd.,  
Kyiv 03142, Ukraine*

<sup>3</sup> *National Technical University of Ukraine "Igor Sikorsky Kyiv Polytechnic Institute",  
Prospekt Peremohy 37, Kyiv 03056, Ukraine*

The features of the critical bending of a beam of magneto-active elastomer (MAE) in a transverse uniform magnetic field have been studied. It is shown that the critical bending of the beam induced by the magnetic field is accompanied by a spontaneous change in the magnetic symmetry of the MAE. Due to the strong magnetoelastic coupling in the MAE, the critical bending induced by the magnetic field occurs as a magnetoelastic phase transition, which is characterized by the critical behaviour of interconnected bending and a critical change in the effective magnetization of the MAE.

It was found that a beam bend in magnetic field takes place mainly as an elastic deformation, although a small plastic one has place too. It was found that in the case obtains of the full loop of magnetization reversal the longitudinal residual magnetization after first magnetization eliminates the uncertainty for the bending direction in a transverse magnetic field of the MAE beam, which has some coercivity.

In the weak fields the bending turns out directly proportional to the strength of the magnetic field, due to this residual magnetization, and an inversion of the bending direction takes place together with change of the magnetic field direction. For a beam with such coercivity MAE, the critical bending behaviour is preserved, but during the input/output of the magnetic field, the magnetic field modules of the critical points positions on the "up" and "down" curves do not coincide. The shift of critical points is caused by the small residual bending - plastic deformation of the beam that presents after previous bending [1]. For the beam with practically absence of the coercivity the bending direction does not change with changing of the magnetic field sign in the magnetic reversal process due to this residual bending.

These results are of practical importance in applications of MAE as executive mechanisms controlled by an external magnetic field, for example, for soft robotics.

1. Kalita V. M., Dzhezherya Yu. I., Cherepov S. V., Skirta Yu. B., Bodnaruk A. V., Ryabchenko S. M.. Spontaneous change of symmetry in a magnetoactive elastomer beam at its critical bending induced by a magnetic field// Smart Mater. Struct. -2023. -Vol.32. -P.045002.

# Electric field impact on the electrocaloric and dielectric response of the ferroelectric BaTiO<sub>3</sub> – WS<sub>2</sub> – Ag nanocomposites

Anna N. Morozovska<sup>1</sup>, Oleksandr S. Pylypchuk<sup>1</sup>, Andrii V. Bodnaruk<sup>1</sup>, Hanna V. Shevliakova<sup>2</sup>, Serhii Ivanchenko<sup>3</sup>, Lesya P. Yurchenko<sup>3</sup>, Eugene A. Eliseev<sup>3</sup>, Nicholas V. Morozovsky<sup>1</sup> and Victor V. Vainberg<sup>1</sup>

<sup>1</sup> *Institute of Physics, National Academy of Sciences of Ukraine, 46, pr. Nauky, 03028 Kyiv, Ukraine*

<sup>3</sup> *Department of Microelectronics, National Technical University of Ukraine “Igor Sikorsky Kyiv Polytechnic Institute”, Kyiv, Ukraine*

<sup>3</sup> *Institute for Problems of Materials Science, National Academy of Sciences of Ukraine, Krjijanovskogo 3, 03142 Kyiv, Ukraine*

Using Landau-Ginzburg-Devonshire approach we have calculated the electric field dependence of the polarization, pyroelectric and dielectric responses, and the electrocaloric temperature change of the strained ferroelectric BaTiO<sub>3</sub> core-shell nanoparticles. We predict that compressive strains suppress the ferroelectric polarization and can induce the paraelectric state; and tensile strains increase the polarization and support the ferroelectric state in the BaTiO<sub>3</sub> core.

The electrocaloric response of a ferroelectric composite consisting of the core-shell BaTiO<sub>3</sub> nanoparticles, semiconducting WS<sub>2</sub> nanoparticles and Ag nanoparticles incorporated in a heat conductive media has been calculated and analyzed. We obtain that to reach the maximal electrocaloric response, it makes sense to prepare dense composites with BaTiO<sub>3</sub> nanoparticles volume ratio about or more than 30%, and to use polymers and/or fillers with less heat mass than the nanoparticles. It is also useful to incorporate fillers with low heat conductance, such as WS<sub>2</sub> nanoparticles and/or Ag nanoparticles, which can act as heat sinks and thus facilitate the heat transfer from the ferroelectric nanoparticles to the external environment.

We prepared the dense composites consisting of (28 – 35) vol.% of the BaTiO<sub>3</sub> nanoparticles incorporated in different organic polymers, WS<sub>2</sub> or Ag nanoparticles (as diffused from the silver paste) and performed measurements of the capacitance-voltage and current-voltage characteristics of the composites. The semiconducting WS<sub>2</sub> and metallic Ag nanoparticles effectively screen the polarization of BaTiO<sub>3</sub> nanoparticles and can induce inhomogeneous electric field inside the BaTiO<sub>3</sub> nanoparticles. Also, the enhancement of the local fields outside the semiconducting or metallic nanoparticles may be very high and lead to the electric breakdown of the composite, which was observed experimentally.

Acknowledgements. A.N.M., O.S.P. and A.V.B. acknowledge the support from the National Research Fund of Ukraine (project “Low-dimensional graphene-like transition metal dichalcogenides with controllable polar and electronic properties for advanced nanoelectronics and biomedical applications”, grant application 2020.02/0027). This research (L.P.Y. and S.I.) is sponsored by the NATO Science for Peace and Security Programme under grant SPS G5980 “FRAPCOM”.

# Heat capacity and thermal expansion: analyzing of atomic, molecular crystals and carbon nanostructure systems.

M. S. Barabashko<sup>1</sup>, R. M. Basnukaeva<sup>1</sup>, A. I. Krivchikov<sup>1</sup>,

O. A. Korolyuk<sup>1</sup>, A. Jeżowski<sup>2</sup>

<sup>1</sup>*B. Verkin Institute for Low Temperature Physics and Engineering of the National Academy of Sciences of Ukraine, 47 Nauky Ave., Kharkiv 61103, Ukraine*

<sup>2</sup>*Institute for Low Temperatures and Structure Research Polish Academy of Sciences, ul. Okólna 2, Wrocław 50-422, Poland*

The heat capacity  $C_V(T)$  and the volumetric thermal expansion coefficient  $\beta(T)$  are fundamental and important thermodynamic parameters for solids that are widely studied using many theoretical and experimental methods. Studies of heat capacity and thermal expansion are powerful tools for understanding lattice vibrations, phase transitions, tunneling, and quantum effects in ordered and disordered systems.

The aim of this study is to analyze the data of heat capacity and thermal expansion of crystalline and amorphous materials to determine the influence of the manifestation of the structure of solids on the proportional dependence between  $C_V(T)$  and  $\beta(T)$ . We considered the systems of xenon atoms adsorbed on the surface of carbon nanotubes, atomic (Xe, Ar) and molecular cryocrystals (N<sub>2</sub>, CO<sub>2</sub>, CO, N<sub>2</sub>O) and carbon nanostructures with a complex phonon spectrum. In both cases of the system of compacted nanotubes SWCNTs and fullerite C<sub>60</sub>, it is possible to propose a generalized linear function between  $\beta/\beta^*$  ratio and  $C_V/R$ , where  $\beta^*$  is the normalization parameter for the coefficient of volumetric thermal expansion and R is the universal gas constant. Deviations from this function indicate anomalies in  $\beta/\beta^*$  vs.  $C_V/R$ , which appear for experimental data. To explain the proportional correlation observed for simple atomic and molecular crystals, we analyzed new experimental results of the universal behavior of the low-temperature heat capacity of molecular crystals. It was found that all frequencies of the real spectrum are proportional to the frequency  $\omega_{vH}$  of the first van Hove singularity, the magnitude of which depends on the volume. Therefore, the Grüneisen parameter becomes the same for all modes. Note that the facts discussed above can explain the proportional correlation between heat capacity and thermal expansion for crystals with appear the first Van Hove feature in the density of vibrational states. In the case of strongly anisotropic solids, the first van Hove feature is not realized in the density of vibrational states, and in this case, there is no condition for realizing a proportional correlation at lower temperatures between heat capacity and thermal expansion.

## ACKNOWLEDGMENTS

The work was supported by the National Research Foundation of Ukraine (NRFU project No. 2020.02/0094).

# Features of NiC formation at mechanical alloying of the equimolar Ni-CNT and Ni-Graphite mixtures

Belyavina N.M., Ostapenko R.V., Kuryliuk A.M., Nakonechna O.I.

*Taras Shevchenko National University of Kyiv, Ukraine*

As a result of systematic studies of the tested samples obtained by mechanical alloying (MA) of the Ni-carbon nanotubes (CNT) and Ni-Graphite mixtures, we have shown that the interaction of nickel with CNT or graphite leads to the formation of NiC<sub>x</sub> phase. It has been established that at the initial stage of the MA the NiC<sub>x</sub> compound developed has a defective ZnS-sfalerite structure, which is internally deformed to make the NiC with further processing. The magnetic properties of the mechanically alloyed powder NiC and the hardness of sintered under high pressure and high temperature (HPHT) NiC compacts show certain differences depending on the form of the carbon used in the charge [1].

Equimolar Ni-CNT and Ni-Graphite mixtures were simultaneously milled in a high-energy planetary mill. The test samples taken after every 60 min of processing were examined by X-ray diffraction analysis methods with total refinement of the NiC<sub>x</sub> crystal structure. The results of these calculations are presented as the dependences of the number of carbon atoms embedded in the nickel lattice during MA ( $N_C$ ) (Fig.)

Analysis of the experimental data (Fig.) reveals that the plot of  $N_C$  vs MA time ( $t$ ) is fitted well by the following equation:  $N_C = A[1 - \exp(-kt)]$ , where  $A$  and  $k$  are constants. Here:  $A = 8.351$  and  $k = 0.000875$  for Ni-CNT mixture, and  $A = 5.933$  and  $k = 0.001710$  for Ni-Graphite mixture. By analogy with the oxidation process, the  $A$  constant could be associated with the number of vacancies, available for placement of the CNT or graphite, and the  $k$  constant characterizes the rate of MA. Different impact of CNT and graphite on mechanical alloying of Ni-carbon charge is discussed.

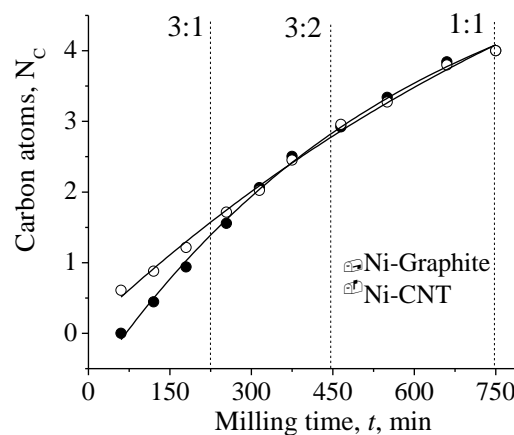


Fig. Dependences of the number of carbon atoms in the NiC<sub>x</sub> lattice on the MA treatment time.

This work has been supported by the Ministry of Education and Science of Ukraine: Grant of the Ministry of Education and Science of Ukraine for the prospective development of the scientific direction "Mathematical sciences and natural sciences" at Taras Shevchenko National University of Kyiv.

1. R. Ostapenko, K. Ivanenko, A. Kuryliuk, O. Nakonechna, N. Belyavina. Synthesis and characterization of the novel nanostructured NiC carbide obtained by mechanical alloying. //Advanced Powder Technology. – 2022. – T. 33. – №. 2. – C. 103390.

# Вплив розміру і властивостей шару діелектрика на поверхневий плазмонний резонанс в 1D-структурах

Карандась Я.В.<sup>1</sup>, Коротун А.В.<sup>1,2</sup>, Рева В.І.<sup>1</sup>

<sup>1</sup>Національний університет «Запорізька політехніка», Україна

<sup>2</sup>Інститут металофізики ім. Г. В. Курдюмова НАН України, Україна

Металеві 1D-структури є привабливими з точки зору застосування у біології і медицині, оскільки за рахунок налаштування їх геометричних параметрів частота поздовжнього поверхневого плазмонного резонансу (ППР) може попадати у так звані біологічні вікна прозорості. Проте, такі наноструктури мають суттєвий недолік – ускладнення прищеплення рецепторів, необхідних, зокрема, для роботи ППР-сенсорів. Покриття поверхні наноструктури діелектричною оболонкою усуває цю проблему, надаючи вказаним наноструктурам біологічної сумісності. З огляду на вищевказане, задача про визначення частот ППР метал-діелектричних 1D-структур є актуальною.

Частоти поздовжнього (поперечного) ППР можна визначити з умови рівності нулю дійсної частини знаменника виразу для поляризованості метал-діелектричної стрижнеподібної наночастинки. За умови відсутності загасання матимемо

$$\omega_{sp}^{\perp(\parallel)} = \frac{\omega_p}{\sqrt{\epsilon^\infty + \mathcal{L}_{\perp(\parallel)} \epsilon_s}}, \quad (1)$$

де  $\omega_p$  – плазмова частота;  $\epsilon^\infty$  – внесок кристалічної ґратки в діелектричну функцію;  $\epsilon_s$  – проникність діелектрика оболонки;

$$\mathcal{L}_{\perp(\parallel)} = \frac{\mathcal{A}_{\perp(\parallel)}}{1 + \mathcal{A}_{\perp(\parallel)} \left( \mathcal{L}_{\perp(\parallel)}^{(1)} - \beta_c \mathcal{L}_{\perp(\parallel)}^{(2)} \right)} - 1, \quad (2)$$

а

$$\mathcal{A}_{\perp(\parallel)} = \frac{1}{\beta_c} \left( 1 + \frac{1 - \mathcal{L}_{\perp(\parallel)}^{(2)}}{\mathcal{L}_{\perp(\parallel)}^{(2)}} \frac{\epsilon_m}{\epsilon_s} \right). \quad (3)$$

У формулах (2) і (3)  $\epsilon_m$  – діелектрична проникність оточуючого середовища;  $\beta_c$  – об'ємний вміст металевої фракції у наночастинці;  $\mathcal{L}_{\perp(\parallel)}^{(1,2)}$  – фактори деполяризації металевого осердя і всієї наночастинки, які залежать від її розмірів.

Співвідношення (1) – (3) дозволяють визначити залежність частот поздовжнього (поперечного) ППР та вплив на ці частоти діелектричної проникності та розмірів оболонки.

# Плазмонні заборонені зони в нанокompозиті з хаотично розташованими металевими сфероїдальними включеннями

Павлище Н.І.<sup>1</sup>, Коротун А.В.<sup>1,2</sup>, Тітов І.М.<sup>3</sup>

<sup>1</sup>Національний університет «Запорізька політехніка», Україна

<sup>2</sup>Інститут металофізики ім. Г. В. Курдюмова НАН України, Україна

<sup>3</sup>UAD Systems, Україна

Оптичні властивості невпорядкованих композитів із металевими нанорозмірними включеннями активно досліджуються з метою більш глибокого розуміння процесів поширення електромагнітних хвиль на поверхні таких композитів та їх ефективного практичного використання у нанофотонних технологіях.

У склометалевих композитах під дією лазерного випромінювання сферичні металеві включення можуть деформуватися у сфероїдальні. Тому дослідження електромагнітних хвиль на поверхні композитів є актуальною задачею. У випадку малої концентрації металевих включень ефективна діелектрична функція досліджуваного композиту має вигляд:

$$\epsilon_{\text{eff}} = \frac{(1-\beta)\epsilon_m + \beta\mathfrak{G}(\omega)}{1-\beta + \beta\mathfrak{G}}, \quad (1)$$

де  $\epsilon_m$  – проникність діелектричної матриці;  $\beta$  – об’ємний вміст металевих включень;

$$\mathfrak{G} = \frac{\epsilon_m}{3} \left( \frac{2}{\epsilon_m + \mathcal{L}_{\perp}(\epsilon(\omega) - \epsilon_m)} + \frac{1}{\epsilon_m + \mathcal{L}_{\parallel}(\epsilon(\omega) - \epsilon_m)} \right), \quad (2)$$

$\mathcal{L}_{\perp(\parallel)}$  – фактори деполяризації; діелектрична функція матеріалу частинок-включень (за відсутності загасання)

$$\epsilon(\omega) = \epsilon^{\infty} - \frac{\omega_p^2}{\omega^2}, \quad (3)$$

де  $\omega_p$  – плазмова частота;  $\epsilon^{\infty}$  – внесок кристалічної ґратки в діелектричну функцію.

З урахуванням співвідношень (2) і (3), з виразу (1) можна одержати частотну залежність ефективної діелектричної функції композиту

$$\epsilon_{\text{eff}}(\Omega) = \epsilon_m \frac{\Omega_{\text{TO}_1}^2 \Omega_{\text{TO}_2}^2 (\Omega^2 - \Omega_{\text{LO}_1}^2)(\Omega^2 - \Omega_{\text{LO}_2}^2)}{\Omega_{\text{LO}_1}^2 \Omega_{\text{LO}_2}^2 (\Omega^2 - \Omega_{\text{TO}_1}^2)(\Omega^2 - \Omega_{\text{TO}_2}^2)}, \quad (4)$$

де  $\Omega = \omega/\omega_p$ , а  $\Omega_{\text{LO}_i}$ ,  $\Omega_{\text{TO}_i}$  ( $i=1, 2$ ) – частоти поздовжніх і поперечних оптичних мод, які залежать від  $\beta$ ,  $\mathcal{L}_{\perp(\parallel)}$ ,  $\epsilon_m$  та  $\epsilon^{\infty}$ .

Співвідношення (4) дозволяє побудувати плазмонні заборонені зони, тобто частотні інтервали, в яких неможливе існування поверхневих плазмон-поляритонів.

## **Швидкість загасання поверхневих плазмонних резонансів у сферичних металевих оболонках змінної товщини**

Малиш Р.О.<sup>1</sup>, Коротун А.В.<sup>1,2</sup>, Рева В.І.<sup>1</sup>, Тітов І.М.<sup>3</sup>

<sup>1</sup>Національний університет «Запорізька політехніка», Україна

<sup>2</sup>Інститут металофізики ім. Г. В. Курдюмова НАН України, Україна

<sup>3</sup>UAD Systems, Україна

Плазмонні явища в наночастинках різного складу, структури і геометрії з огляду на їх широке практичне застосування у різних галузях людської діяльності викликають значний інтерес. Потрібно відзначити, що залежності частот поверхневого плазмонного резонансу (ППР) від форми, складу, структури і розмірів наночастинок та властивостей оточуючого діелектричного середовища добре вивчені. Проте, крім спектрального положення ППР, який визначається вищезгаданою частотою, важливою характеристикою лінії ППР є її півширина, що визначається швидкістю загасання резонансів. В свою чергу, у швидкість загасання дають адитивний внесок три механізми: об'ємна та поверхнева релаксація і радіаційне загасання. Якщо величину швидкості об'ємної релаксації можна вважати постійною, то швидкості поверхневої релаксації та радіаційного загасання можуть залежати від частоти світла та геометричних параметрів наночастинок.

Загальним підходом до визначення швидкостей поверхневої релаксації та радіаційного загасання є кінетичний підхід, згідно з яким провідність (або діагональні компоненти тензора провідності) визначається в результаті розв'язку рівняння Больцмана, а швидкість поверхневої релаксації та радіаційного загасання пропорційні дійсній частині провідності. Проте, треба відзначити, що вищевказаний підхід був застосований лише для монометалевих сферичних та сфероїдальних наночастинок [1]. Тому поширення кінетичного підходу для визначення півщини лінії ППР оболонкових наночастинок є актуальною задачею.

В роботі одержано вирази для швидкостей поверхневої релаксації та радіаційного загасання ППР у сферичних оболонках змінної товщини. Показано, що вказані величини залежать не лише від частот світла та радіусів неконцентричних сфер, а і від відстані між їх центрами. Проведено порівняння з випадком сферичної металевої оболонки постійної товщини.

1. P.M. Tomchuk, D.V. Butenko. Dependences of dipole plasmon resonance damping constants on the shape of metallic nanoparticles// Ukr. J. Phys. - 2015. - Vol.60. -P.1042-1048.

# Ionic conductivity in single-crystalline and amorphous lithium germano-germanates

A.O. Diachenko, M.P. Trubitsyn, M.D. Volnianskii,

M.M. Koptiev, Ye.V. Skrypnik

*Oles Honchar Dnipro National University, Ukraine*

Structural disorder is one of the main conditions for fast ionic transport in solid electrolytes. Violations of long-range order, appearance of host atoms vacancies and/or interstitials, iso- or heterovalent doping cause structural disordering in crystalline media. The crystals of lithium/sodium germano-germanates  $\text{Li}(\text{Na})_2\text{O}-x\text{GeO}_2$  have framework structures and represent available matrixes to design new ionic conductors. Germanium-oxygen octahedral and tetrahedral groups are linked by common edges or vertices and form the structural skeletons of  $\text{Li}(\text{Na})_2\text{O}-x\text{GeO}_2$  crystals. Light  $\text{Li}^+(\text{Na}^+)$  ions are weakly bound to germanium-oxygen frame and occupy the sites within the structural channels. Hopping of  $\text{Li}^+$  ions through the quasi-equilibrium interstitial positions within the channels provides for high ionic conductivity in an external electric field.

Here we report the comparative analysis of the effects of structural disorder and heterovalent doping on ionic conductivity in single-crystalline and amorphous lithium-sodium tetragermanate ( $\text{LiNaGe}_4\text{O}_9$ ,  $x=4$ ) and lithium heptagermanate ( $\text{Li}_2\text{Ge}_7\text{O}_{15}$ ,  $x=7$ ) [1, 2]. It is shown that for the glasses of the both compounds conductivity increases in one-three orders as compared with the single crystals. Preparation of the nanometer scaled glass-ceramics allows to further increase conductivity of lithium heptagermanate. The opposite situation is observed for lithium-sodium tetragermanate. Conductivity of glass-ceramics decreases in one-two orders of magnitude as compared with the glass. Heterovalent doping with  $\text{Cr}^{3+}$ ,  $\text{Al}^{3+}$ ,  $\text{Mn}^{2+}$ ,  $\text{Gd}^{3+}$  strongly influence ionic conductivity in the single crystals of the both compounds. The doping effects are explained by appearance of Li interstitials or vacancies which act as the charge compensators of the foreign ions. In the glasses and nanostructured glass-ceramics number of weakly bound Li ions increases sharply and, accordingly, the effect of doping on conductivity is greatly weakened.

1. A.O. Diachenko, M.P. Trubitsyn, M.D. Volnianskii, I. Jankowska-Sumara, Y.V. Skrypnik, M.M. Koptiev. Glass devitrification and electrical properties of  $\text{LiNaGe}_4\text{O}_9$ // *Molecular Crystals and Liquid Crystals*. – 2021. – Vol.721, issue 1. – P.10–16.
2. M. Trubitsyn, M. Koptiev, M. Volnianskii. Ionic Conductivity in Single Crystals, Amorphous and Nanocrystalline  $\text{Li}_2\text{Ge}_7\text{O}_{15}$  Doped with Cr, Mn, Cu, Al, Gd// *Springer Proc. in Phys.* – 2023. – Vol 279. – P. 585–598.



# **Multi-walled carbon nanotube network on porous silicon for humidity sensing**

Olenych I.B., Pavlyk M.R., Serkiz R.Ya.

*Ivan Franko National University of Lviv, Ukraine*

The trend of miniaturization of sensor devices is dominant due to the coordinated development of nanomaterials and technologies. Carbon nanotubes (CNTs) have become one of the most popular and widely used starting nanomaterials in sensor electronics. CNTs have attracted a large number of studies due to their high potential for NO<sub>2</sub> and hydrogen-containing molecule sensing [1]. To increase the sensitivity and selectivity of super-miniaturized chemical sensors, CNTs are often combined with other nanomaterials. In particular, hybrid structures of CNTs and porous silicon (PS) as a host matrix for nanotube deposition may offer significant improvement of sensory properties due to the large surface area of the PS. Besides, PS-based structures have also been found useful in gas-sensing systems [2].

We proposed a two-component system to fabricate humidity sensor elements using simple and low-cost techniques. The PS layer with a branched pore system was obtained by electrochemical etching of a silicon wafer in hydrofluoric acid. An aqueous suspension of multi-walled CNTs (mw-CNTs) was deposited on the PS surface. After drying in the air, a disordered network of mw-CNTs was formed on the surface and in the pores of the PS. The nanotube network on a silicon substrate with an oxide layer was also formed to study the influence of the porous host matrix on the sensory properties of mw-CNTs. The morphology of the obtained structures was characterized by SEM. The study of the electrical parameters of experimental samples was carried out in both DC and AC modes. A decrease in the resistance of the mw-CNT network on the PS layer compared with one on the silicon substrate has been found likely due to the formation of more percolation clusters and current paths. In addition, an increase in relative humidity causes an increase in the resistance and the capacitance of obtained sensitive elements. Response time and the sensing ability dependence on the relative humidity were analyzed to estimate the sensory properties of the mw-CNT network on the PS.

1. Y. Wang, J.T.W. Yeow. A Review of Carbon Nanotubes-Based Gas Sensors // *Journal of Sensors*. - 2009. - Vol. 2009. - P. 493904.
2. I.B. Olenych, L.S. Monastyrskii, O.I. Aksimentyeva, Yu.Yu. Horbenko. Multifunctional Hybrid Nanosystems Based on Porous Silicon. In: *Nanoobjects & Nanostructuring*. Vol. I. - Mississauga, Ontario: Nova Printing Inc., 2022. - Chapter 8. - P. 115-143.

# **Badanie struktur wtórnych na powierzchni tarcia powłok eutektycznych układu Fe-Mn-C-B-Si-Ni-Cr**

Pashechko M.

*Technikal University of Lublin*

W pracy przedstawiono badania struktur wtórnych powstających podczas tarcia powłok ze stopu eutektycznego Fe-Mn-C-B-Si-Ni-Cr. Stop eutektyczny zastosowano jako mieszanka rdzeniowa do produkcji drutu proszkowego o średnicy 2,4 mm. Powłoki otrzymano metodą napawania GMA w osłonie CO<sub>2</sub>. Badania tribologiczne prowadzono w układzie trzpień-tarcza przy nacisku jednostkowym 10 MPa w warunkach tarcia suchego. Do badań struktur wtórnych (nanostruktur) na powierzchni tarcia i po głębokości 5, 10, 15, 20, 50, 100, 200, 6000 nm. wykorzystano skaningowy mikroskop elektronowy SEM/EDX oraz rentgenowską spektroskopię fotoelektronów XPS. W procesie tarcia stopu eutektycznego występuje segregacja atomów C, B i Si. Na powierzchni tarcia oraz w warstwie przypowierzchniowej powłoki Fe-Mn-C-B-Si-Ni-Cr stwierdzono obecność takich związków jak tlenki (B<sub>2</sub>O<sub>3</sub>, SiO<sub>2</sub>, Cr<sub>2</sub>O<sub>3</sub>, NiO, FeO, Fe<sub>2</sub>O<sub>3</sub>), węgliki (Fe<sub>3</sub>C, Cr<sub>7</sub>C<sub>3</sub>), borki (FeB, Fe<sub>2</sub>B), a także C-C, C=O, C-O=C, C-H, C-OH, C-O-C. Formowanie się struktur wtórnych (nanostruktur) zwiększa odporność na zużycie powłok trzymywanych ze stopu eutektycznego Fe-Mn-C-B-Si-Ni-Cr.

Słowa kluczowe: powłoki, napawanie, zużycie, segregacja, struktury wtórne.

## Edge Luminescence of CsPbCl<sub>3</sub> Doped Single Crystals

O. Pidhornyi, Ya. Chornodolskyi, A. Pushak, O. Antonyak, T. Demkiv,  
R. Gamernyk, A. Voloshinovskii

*Ivan Franko National University of Lviv, Ukraine*

Organic-inorganic metal halides exhibit excellent optoelectronic properties and are used in photovoltaics and light-emitting devices. These metal halides have the perovskite structure ABX<sub>3</sub>, which consists of octahedral units BX<sub>6</sub>, where the B atom is a divalent metal (usually Sn<sup>2+</sup> or Pb<sup>2+</sup>) and X is a monovalent halide (usually Cl<sup>-</sup>, Br<sup>-</sup> or I<sup>-</sup>); cation A is usually Cs<sup>+</sup> or small organic molecular compounds. Numerous studies have shown the enhancement of edge emission of ABX<sub>3</sub> halide perovskite nanoparticles (A=Cs; B=Pb; X=Cl, Br, I) upon activation with cation ions, which replace Cs<sup>+</sup> or Pb<sup>2+</sup> cations [1]. Yes, for CsPbCl<sub>3</sub> nanoparticles in the case of doping with Cd<sup>2+</sup> or Mg<sup>2+</sup> cations, the luminescence quantum yield increased from ~1% to 100% [2].

The luminescence spectrum of a pure CsPbCl<sub>3</sub> single crystal excited by synchrotron radiation with a photon energy of 8.0 eV exhibits a dominant peak at 416.7 nm with a half-width of 9 meV and a small plateau in the long-wavelength region of the main peak. The emission spectrum is in good agreement with the luminescence spectra reported in previous studies [2]. The peak at 416.7 nm can presumably be interpreted as the luminescence of a free exciton.

The intensity and structure of the luminescence spectrum change when the CsPbCl<sub>3</sub> crystal is activated by cadmium ions. Up to a concentration of 0-0.5 mol % CdCl<sub>2</sub>, the integral intensity of luminescence increases 5 times. There are also additional narrow emission peaks in the long-wavelength region near the free exciton peak at 416.7 nm. For a concentration of 0.5 mol % CdCl<sub>2</sub>, narrow emission peaks were identified at 2.990, 2.976, 2.964, 2.953, and 2.935 eV based on the Gaussian distribution. In the range of 0-0.5 mol % CdCl<sub>2</sub>, the position of the free exciton peak does not change significantly. This allows us to conclude that at these concentrations, impurities do not cause significant changes in the energy structure of the CsPbCl<sub>3</sub> crystal.

Thus, our studies of edge exciton luminescence in a CsPbCl<sub>3</sub> single crystal activated by cadmium ions upon excitation by synchrotron radiation with quantum energy 8 eV demonstrate the possibility of significantly increasing the luminescence intensity upon activation by metal cations.

1. Y. Chen, Y. Liu, M., Hong Cation-doping matters in cesium lead halide perovskite nanocrystals: From physicochemical fundamentals to optoelectronic applications // *Nanoscale*. – 2020. – Vol.12. – P. 12228–12248.
2. A.Voloshinovskii, S. Myagkota, A. Gloskovskii, S.Zazubovich, Luminescence of CsPbCl<sub>3</sub> nanocrystals dispersed in a CsCl crystal under high-energy excitation // *Phys. Stat. Solidi (B)*. – 2001. – Vol.225(1). – P.257–264.

# Hybrid solder joints: Study of the thermophysical properties of solder flux with minor additions of Fe nanoparticles

Yakymovych A.<sup>1,\*</sup>, Khatibi G.<sup>1</sup>, Wodak I.<sup>1</sup>, Goh Y.X.<sup>2</sup>

<sup>1</sup>*Institute of Chemical Technologies and Analytics, TU Wien, Vienna 1060, Austria*

<sup>2</sup>*Department of Mechanical Engineering, Faculty of Engineering, Universiti Malaya, Kuala Lumpur 50603, Malaysia*

The viscosity and contact angle of the flux with minor additions of Fe nanoparticles have been investigated. The produced nanoemulsions consisted of the commercial flux TACFlux 089HF (INDIUM Corporation) and the nanosized Fe powder (Nanografi) by mechanically stirring for about 30 min at room temperature. The content of the added metal nanoparticles varied from 0.0 to 2.0 wt. %.

The share rate and temperature dependencies of the nanocomposite fluxes were investigated by the rotating viscosimeter method (Anton Paar, MCR 300) method. It was found that nanosized Fe particles decrease the viscosity of the solder flux, while the most significant reduction was obtained by the primary addition of 0.5 wt. % Fe NPs. The viscosity exponentially decreases with an increase in the temperature for all samples.

The contact angle of the nanocomposite flux placed on Cu substrate was measured by the sessile drop method. The measurements were performed under Ar flow. The samples were heated up from room temperature to 363K, similar to the viscosity measurements. Images were taken by camera every 10 sec during the whole measurement. The contact angle was determined based on the shape of the sample using the shape-analysis program “drop” [1]. It was found that the contact angle of the flux decreases with the addition of Fe NPs.

In addition, the contact angle of the solder joints produced in a sandwich form solder ball/flux with Fe NPs/Cu substrate was investigated. It was found that the contact angle for the solder joint increased with additions of Fe NPs.

Financial support for this study came from the Austrian Science Fund (FWF) under Project No. P34894 and from Austria’s Agency for Education and Internationalisation (OeAD) under Project ASEA-UNINET / 2022-2023 / TU Wien / 3.

[1] Gruner S, Kohler M, Hoyer W (2009) J Alloys Compd 482:335

# Magnetoresistance and Hall effect caused by Berry curvature in $\text{Sr}_2\text{FeMoO}_6$ double perovskite

Konoplyuk S.M., Krupa M.M.

*Institute of magnetism of NASU and MESU, Kyiv, Ukraine*

The  $\text{Sr}_2\text{FeMoO}_6$  is ferrimagnet with high Curie temperature and full spin polarization, which is considered as a prospective candidate for spintronic applications, in particular, as spin injector and material for MRAM and magnetic sensors. In spite of its attractive properties, technology of  $\text{Sr}_2\text{FeMoO}_6$  synthesis is complex and search for routes to improve materials characteristics especially transport ones is under way. Here, magnetoresistance on the strontium ferromolybdate specimens prepared by citrate-gel method from nanopowders followed by compacting and thermal treatment at different regimes was studied. The Hall effect was calculated by *ab initio* approach using Quantum Espresso and Wannier90 software packages.

The study confirmed high sensitivity of  $\text{Sr}_2\text{FeMoO}_6$  to the processing parameters such as pressure and temperature of powder compacting as well as temperature and duration of followed annealing in Ar atmosphere. The optimal regime of compacting allowed to avoid cracking involved pressing under 4 GPa at  $T=800$  K. Further heat treatment of compacted specimens in Ar atmosphere have shown that three types of electric conductivity: metallic, semiconducting and mixed ones can be obtained in the  $\text{Sr}_2\text{FeMoO}_6$  specimens depending on annealing time. The highest magnitude of magnetoresistance was found in the semiconducting specimen (about 44 %), while the specimen with metallic type demonstrated magnetoresistance of about 21 %. The elevated values of magnetoresistance in the semiconducting specimen were achieved due to conduction mechanism related to tunneling through intergrain dielectric layers formed by secondary  $\text{SrMoO}_4$  phase.

The Hall effect was computed by constructing of the Hamiltonian in the maximally localized Wannier functions basis. Calculations of the Berry curvature, which is origin of high intrinsic Hall effect showed that its highest magnitudes concentrate between  $\Gamma$  and N high-symmetry points in Brillouin zone near avoided band crossings. The Hall conductivity calculated by integrating the Berry curvature over all occupied bands was found to be  $\sim 22$  S/cm. Strong enhancing the Berry curvature above Fermi level indicates possibility to yield much higher Hall effect by proper tuning strontium ferromolybdate composition.

## **Magnetic properties of thin films of the Gd-Fe system.**

Prysyazhnyuk V.I.

*Ivan Franko National University of Lviv, Ukraine*

Amorphous films of double compounds of the Gd-Fe system were obtained by thermal evaporation on fluoroplastic substrates. The substrate temperature was 293K. An increase in the temperature of the substrate or annealing of the films leads to an increase in the proportion of the polycrystalline phase. The film thickness of the investigated films was 200 nm. Checking the structure of the films was carried out on a UEMV-100K electron microscope using a PRON-2 high-temperature attachment. Magnetic measurements were carried out on the original vibrating magnetometer. The field magnetization vector was parallel to the plane of the film, the maximum saturating field was 300 KA/m.

Magnetic characteristics of films and massive compounds of the Gd-Fe system (GdFe<sub>2</sub>, GdFe<sub>5</sub> and Gd<sub>2</sub>Fe<sub>17</sub>) were measured.

Magnetic hysteresis loops with small work of the external field on remagnetization were obtained. Such loops are characteristic of soft-magnet ferromagnets.

The value of the coercive force is determined. It was established that the coercive force decreases during the formation of amorphous films in comparison with massive samples. This is due to the absence of long-range order in amorphous materials and, as a result, much smaller magnetic anisotropy, which in turn leads to a small coercive field. The formation of the polycrystalline phase in the films leads to the fact that our samples become more magnetically hard, even compared to massive samples. This is explained by the fact that we measured the magnetization of the films along their surface. And it is known that there are flat domains in films, which are much easier to magnetize along than perpendicular to the surface. We have also established that the coercive force value does not matter how the film crystallization occurs, whether in the process of forming the film itself on heated substrates, or in the process of annealing amorphous films after they are obtained.

Temperature dependences of magnetic saturation for massive compounds and films of GdFe<sub>2</sub> and Gd<sub>2</sub>Fe<sub>17</sub> were obtained. The Curie temperature was established for these compounds. It was found that the structural disorder leads to a decrease in the Curie temperature and the value of magnetic saturation.

## **Flooding processes in the Gd-Fe system**

Prysyazhnyuk V.I.

*Ivan Franko National University of Lviv, Ukraine*

In contemporary materials science, a new direction of chemical-thermal treatment of metals is intensively evolving, involving the use of hydrogen as a technological medium in the processing of functional materials. These hydrogen-based technologies are based on the effects of hydrogen on phase transformations in metals, including polymorphism, atomic ordering, and the formation and decomposition of intermetallic phases and hydrides. A well-known process that influences the formation of the phase-structural state of a material is HDDR (hydrogenation, disproportionation, desorption, recombination). Completing the HDDR process at different stages can yield a wide range of results.

Compounds and films of Gd-Fe<sub>2</sub> were used for the investigation, employing two hydrogenation schemes: Crushed Gd-Fe<sub>2</sub> samples were subjected to a pressure of  $2 \cdot 10^6$  Pa for 168 hours at room temperature. In this first case, hydrogen penetrated the lattice, causing deformation. The amount of absorbed hydrogen depended on the fineness of our powder; in the case of thin films, the quantity of absorbed hydrogen significantly increased compared to the mass of the "absorber." Electron microscopy of the films before and after hydrogenation indicated that these films became more finely dispersed. Upon heating the hydrogenated samples, a reverse process of hydrogen release was observed, as evidenced by the chemical analysis of the chamber air during heating. A potential application of such multilayer structures is the development of hydrogen storage systems. In the second case, hydrogen reacted with Gd-Fe<sub>2</sub>, resulting in the formation of GdH<sub>2</sub> and GdH<sub>3</sub>, along with free iron. This was indicated by the disintegration of the sample (turning into powder) and X-ray studies.

Regrettably, the second method is not very productive for films. However, this hydrogen treatment can be used to impact the magnetic properties of the obtained powders since it forms anisotropic structures in magnetic materials.

## Секція 6

### *Комп'ютерне моделювання неупорядкованих систем.*

#### ***Ab initio* molecular dynamics simulation of Co-Sn melts**

Kashyrina Ya.O., Muratov A.S., Roik O.S.

*Taras Shevchenko National University of Kyiv, Ukraine*

Co-Sn-based alloys have many applications in the production of lead-free soldering, tribological materials, metallic glasses, electroplating, and anode materials in lithium-ion batteries. The experimental X-ray diffraction studies [1,2] reported a significant transformation of the SRO of the Co-Sn melts with concentration. For example, the concentration dependence of the nearest neighbour distance in Co-Sn melts has alternating deviations from additivity: positive for Sn-rich melts and negative for Co-rich melts.

*Ab initio* MD simulation was carried out with compositions  $\text{Co}_{100-x}\text{Sn}_x$  (where  $x = 0, 8, 16, 24, 32, 40, 50, 67, 80, 90$  and  $100$  at.%) at  $650\text{-}1600$  °C range. The *ab initio* calculations were performed under the frame of density functional theory (DFT), with the Vienna *ab-initio* Simulation Package (VASP) using generalized gradient approximation (GGA) parameterized by Perdew-Burke-Ernzerhof exchange and correlation functional (PBE). Projector augmented wave (PAW) pseudopotential of Co and Sn with valence electrons of  $3d^8 4s^1$  and  $5s^2 5p^2$ , respectively, were adapted with the cut-off energy of  $520$  eV. The supercell consists of  $500$  atoms with a size, which correspond to the experimental density. A  $1 \times 1 \times 1$  k-point mesh was used for Brillouin zone sampling. All calculations reached the absolute energy convergence to better than  $10^{-5}$  eV/atom. The MD timestep was  $3$  fs.

Calculated from *ab initio* MD simulation radial distribution functions (RDF) of Co-Sn melts gives a satisfactory agreement with experimental diffraction data [1] (Fig.1). The partial SRO of binary melts has been investigated in detail. The concentration dependence of partial pair distribution functions, structure factors, nearest neighbour distances, and coordination numbers have been discussed. It was observed that the coordination of around Co is independent from pair atom, but Sn formed regions with monoatomic environment.



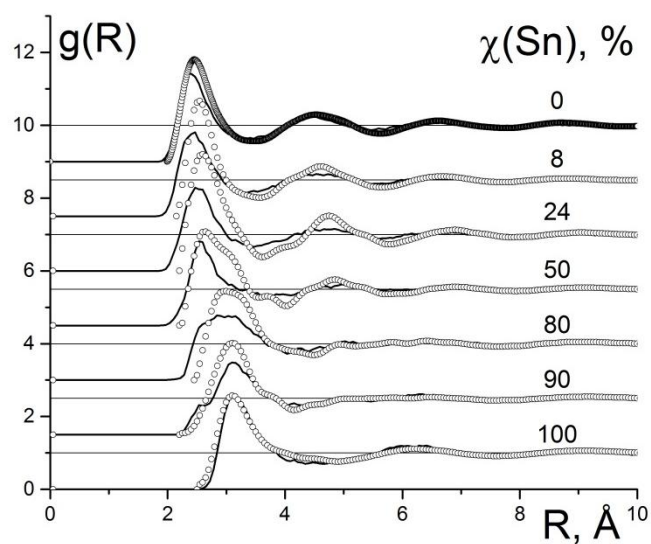


Fig 1. Comparison of experimental ( $\circ$ ) and modeled curves of RDF.

1. V. Kazimirov, O. Roik, V. Sokolskii Structural features of Co-Si, Co-Ge, and Co-Sn binary melts // *Rasplavy*. - 2008. - P. 13-21.
2. A. Yakymovych, I. Shtablavyi, S. Mudry, Structural studies of liquid Co-Sn alloys// *J. Alloys Compd.* -2014. – Vol.610. – P. 438-442.

# Calculation of the speed of sound in liquid Fe at high pressures via molecular dynamics simulations

Demchuk T., Bryk T.

*Institute for Condensed Matter Physics, Lviv, Ukraine*

Current knowledge about the properties of the inner layers of the Earth is based mainly on the results of seismological research. It is known that the Earth's outer core consists of molten iron with a small amount of impurities. Understanding the dynamic properties of iron melts under high pressure and temperature conditions is crucial for advancing our comprehension of the Earth's interior. Recent research on liquid Fe by x-ray diffraction and inelastic x-ray scattering demonstrated that by determining the density and sound velocity of the system at various thermodynamic points, an equation of state for the system can be established and extrapolated to the extremely high-pressure range [1]. This equation of state serves as the basis to develop a model for Earth's internal layers and to compare the properties of the obtained model with data from seismic studies. However, ensuring the accuracy of experimental results remains a crucial challenge. One of the possible solutions is to provide a computer experiment to improve the results.

In this study, we focus on calculating the sound velocity of iron melt at a temperature of 2700 K and a pressure of 44.9 GPa using molecular dynamics simulations. The simulations utilized an EAM-potential, whose parameters were taken from [2], effectively reproducing the properties of liquid iron. Time correlation functions of the longitudinal current were calculated using particles trajectories and velocities data. The peak frequency on the spectrum of such a function corresponds to the propagation frequency of longitudinal collective excitations. By calculating the values of such frequencies for different values of the wave number, the dispersion of acoustic excitations in the system was obtained. The resulting curve agrees well with the dispersion obtained experimentally in [1]. The calculation of the speed of sound was carried out using the new methodology, which allows one to calculate the adiabatic speed of sound knowing the density, the high-frequency speed of sound and the value of the autocorrelation function of the longitudinal stress at zero time. Calculated from the computer experiment value of the speed of sound is 10% lower than the experimental value. This indicates a possible inaccuracy in the calculations of the equation of state of iron and the model of the Earth's outer core.

1. Y.Kuwayama *et al.* Equation of State of Liquid Iron under Extreme Conditions // *Phys. Rev. Lett.* -2020. -Vol.124. -P.165701-1.
2. M.Mendelev *et al.* Development of new interatomic potentials appropriate for crystalline and liquid iron // *Philosophical Magazine.* -2003. -Vol.83. -P.3977–3994.

# Electronic properties of Mn<sup>2+</sup> doped $\beta$ -LiNH<sub>4</sub>SO<sub>4</sub> crystals

Brezvin R.S., Shapravskiy A.O., Stadnyk V.Yo., Shchepanskyi P.A.

*Ivan Franko National University of Lviv, Ukraine*

Lithium ammonium sulfate, LiNH<sub>4</sub>SO<sub>4</sub>, known as LAS, belongs to the M<sub>I</sub>M<sub>II</sub>BX<sub>4</sub> family of ionic crystals, where M<sub>I</sub> is Li, Na, M<sub>II</sub> are Na, K, Rb, Cs atoms or NH<sub>4</sub>, N<sub>2</sub>H<sub>5</sub> molecules, and BX<sub>4</sub> are SO<sub>4</sub>, SeO<sub>4</sub>, and BeF<sub>4</sub> molecules. LAS have two possible modifications ( $\alpha$ -LAS and  $\beta$ -LAS), which can be obtained by slow evaporation of water from aqueous solutions of LiNH<sub>4</sub>SO<sub>4</sub> at different constant temperatures. An important method of material modification is the introduction of impurities of various nature into the structure. The purpose of this study is a theoretical study of the effect of manganese admixture on the electronic structure of the material.

Calculations of the band energy structure and dielectric function were performed within the framework of density functional theory (DFT) using the CASTEP program, which is commonly used in the study of semiconductor and dielectric crystals. Calculations were performed self-consistently, using the Born-Oppenheimer approximation. A generalized gradient approximation (GGA) with Perdew-Burke-Ernzerhof (PBE) parameterization was used to describe the exchange-correlation interaction. The cut-off energy of the plane waves was 400 eV. The effect of the core electrons on valence system has been described by Vanderbilt's ultrasoft pseudopotential. Impurity modeling was performed using the supercell method. A 1×2×2 supercell was used in the calculation, which allowed to simulate the impurity concentration of ~2.3%. The supercell was previously optimized at fixed values of the lattice parameters.

The band-energy structure of LAS crystal with manganese admixture was calculated using the method based on density functional theory. The expansion of energy bands related to the presence of impurities is shown for the crystal. Compared to pure LAS crystal, additional electronic levels corresponding to the manganese impurity states are observed in the band gap. A more detailed analysis of the partial density of electronic states of impurity LAS showed that the manganese *d*-states split by the crystal field form two localized sublevels in the band gap at a distance of approximately 0.6 eV. The *p*-states of Mn are localized in the conduction band, while the levels of *s*-electrons form two local sublevels near the bottom of the conduction band.

The calculated spectral dependence of the dielectric function for principal directions of  $\beta$ -LAS:Mn<sup>2+</sup> reveals a significant anisotropy and additional peaks in the  $\epsilon(\omega)$  spectrum associated with Mn impurity levels.

*Acknowledgments:* The study was performed within the framework of the project 2020.02/0211 of the National Research Foundation of Ukraine “Experimental and theoretical study and prediction of the photoelastic properties of crystalline materials for devices of electromagnetic radiation control”.

# **Computer simulations – an efficient tool for deeper understanding of experimental data of metallic melts structure.**

Shtablavyi I.I., Mudry S.I.

*Ivan Franko National University of Lviv, Ukraine*

The liquid state of matter still remains one of the least studied despite significant progress in the development of experimental techniques in recent decades. However, understanding the nature of fluids is important in many modern applications and technologies. In particular, for the improvement of methods of obtaining metal materials by additive technologies, it is important to understand the phenomena that occur in liquid metals during the process of rapid melting and crystallization. There are many more such examples that require information about the structure of melts and its relationship with properties.

As it is known, the main information about the structure of liquids can be obtained by experimental methods using the diffraction of X-rays, electrons or neutrons. As a result of mathematical processing of the results of the experiment, it is possible to obtain probabilistic data on the main structural parameters. In particular, in this way it is possible to determine the most probable distances between atoms and the average values of number of neighbours. However, based only on the analysis of experimental methods, it is possible to obtain limited information about the structure of liquids, especially for two- and multi-component melts.

In this regard, it is important to use other methods to deepen knowledge about the structural features of single- and especially multicomponent liquids. One of these methods is the method of computer simulations of the structure and properties of materials at the atomic level. The most advanced methods of computer simulations of disordered systems are Monte-Carlo and molecular dynamics methods. Information about the potential of interatomic interaction is necessary for modelling by these methods. If the potential of interatomic interaction is difficult to calculate, in this case, experimental data on the structure of the material can be used for its further simulation using the so-called reverse Monte-Carlo method. As a result of the joint analysis of experimental research results and computer simulation data, it is possible to study the structure of liquids in much more detail.

In this work, the results of the study of the structure of metal melts obtained by X-ray diffraction and computer simulation methods were analysed. The strengths and weaknesses of each of these methods are shown. Recommendations are given for investigations the structure of liquids both by experimental methods and by means of computer simulations.

## **Acknowledgment**

This work was supported by the National Research Foundation of Ukraine (Project No 2022.01/0171).

# **Molecular dynamics simulations of the surface structure of materials in liquid and solid-liquid state.**

Shtablavyi I., Plechystyy V., Popiliovskiy N., Kulyk Yu., Sembratovych N., Mudry S.

*Ivan Franko National University of Lviv, Ukraine*

Many technological processes in modern materials science are related to surface interaction as well as surface structure and properties of materials. In particular, this concerns to thin films technologies, crystal grows, liquid phase epitaxy and many other modern technics of materials processing. Among such technologies the most promising are additive methods of materials producing by means of laser sintering of micro- or nanopowders. Laser sintering is accompanied with melting of particles in bulk or surface and subsequent crystallization. In this case the interaction of surface atomic layers occurs, which results in particles sintering. That is why it is of great importance to have detailed information on materials surface structure and properties both in solid and liquid states.

To study the structure of the surface layers of materials, it was proposed to use both experimental and computer simulations methods [1-3]. Experimental methods give us direct information about the static atomic structure of the surface of materials. However, these methods cannot answer questions about the kinetics of atoms on the surface. In this case, the solution to this problem can be done by computer modeling methods, in particular, by the method of molecular dynamics (MD).

In this work, the structure of the surface layers of copper, aluminum, and silicon was investigated using classical MD simulation. The interaction between atoms was taken into account using EAM or MEAM potentials. Pair correlation functions were used for the structure analysis of the surface and solid-liquid interface layers, depending on the distance from the surface. In addition, the distribution of coordination numbers and free volume of surface and bulk atomic layers at different temperatures was studied.

1. G.A. Somorjai and U. Starke. Monolayer surface structure analysis // *Pure & Appl. Chern.* – 1992. – Vol. 64, No. 4. – pp. 509-527.
2. D. Grozea, E. Landree, C. Collazo-Davila, E. Bengu, R. Plass, L.D. Marks. Structural investigations of metal–semiconductor surfaces // *Micron.* – 1999. – 30. – P. 41–49.
3. P. Geysmans and D. Gorse Molecular dynamics study of the solid–liquid interface // *J. Chem. Phys.* – 2000. – Vol. 113, No. 15. – P. 6382-6389.

## **Acknowledgment**

This work was supported by the National Research Foundation of Ukraine (Project No 2022.01/0171).

# The trimers and dimers states in population-imbalanced fermion system

O. Hryhorchak<sup>1</sup>, G. Panochko<sup>2</sup> and V. Pastukhov<sup>1</sup>

<sup>1</sup>*Professor Ivan Vakarchuk Department for Theoretical Physics,  
Ivan Franko National University of Lviv, 12 Drahomanov Str., Lviv, Ukraine*

<sup>2</sup>*Department of Optoelectronics and Information Technologies,  
Ivan Franko National University of Lviv, 107 Tarnavskyj Str., Lviv, Ukraine*

We consider a model of three-component fermions of mass  $m$  loaded in one-dimensional volume  $L$  with periodic boundary conditions. We assume one component of fermions is macroscopically occupied (say, component ‘III’) with density  $n$  and there are exactly two atoms of another species (one of each sorts ‘I’ and ‘II’). In the thermodynamic limit, the properties of host fermions (sort ‘III’) cannot change drastically when few impurities are immersed. Let such a system is to be in the two-body resonance where the two-body scattering lengths diverge and the only interaction between fermions that is taken into account is the short-range three-body one. This system supports the trimer and the medium-induced dimer states, which are analyzed in detail within a field-theoretic approach. In order to distinguish the trimer and dimer phases of the system we perform the calculations of the appropriate three- and two-particle propagators, respectively. In the region of extreme diluteness of the considered system two impurities of sorts ‘I’ and ‘II’ form the trimer which additionally involves one atom from the medium. An important consequence of the macroscopic occupation of the component ‘III’ is the emergence of the induced two-body interaction between impurities. The physics of the system crucially depends on the nature of the effective potential, i.e., sign of the coupling at low energies of colliding impurities. At very low densities  $n$  of host fermions, the induced two-impurity potential is strictly repulsive. Increase of density of sort ‘III’ particles, however, leads to the change of its character to the attractive one. Since the trimer interacts repulsively with ‘III’ particles, by making the system more dense we simultaneously lower the trimer binding energy. Therefore, at some critical magnitude of  $a_3 p_F$  the formation of dimer should be more energetically preferable and the transition from trimer to dimer state of two impurities should be observed. At small densities of host fermions our particle-hole calculations revealed the well-defined trimer state of the system with a slightly modified dispersion relation. The increase of the medium density leads to suppression of trimer state, and the latter completely vanishes at some critical magnitude of interaction  $\ln(|e_3|/\mu) = \ln 6$ . On the other side of phase diagram, where the density of fermions is extremely large  $\ln(\mu/|e_3|) \neq 1$ , the attachment of

a single host atom to form a trimer costs an enormous amount of energy, and the dimer (bipolaron) with the logarithmically vanishing binding energy emerges. This well-defined quasi particle that cannot occur in vacuum possesses an almost Galilean-invariant spectrum with the total mass of two impurities. The decrease of density of the macroscopically-occupied fermions almost totally depletes the dimer as a quasi-particle at  $\ln(|e_3|/\mu) \approx 2 - 4$ . Therefore, one may expect the dimer-trimer transition in this region. It turns out, however, that the dimer state is always energetically more preferable over the trimer state and no transition happens. Our findings – the obtained quasi-particle residues – give confidence in the experimental preparation of both trimers and dimers in low- and high-density limits of the system, respectively.

## Зміст

The structure of ternary $Al_{80-x}M_{20}Sn_x$ ( $M=Fe, Co, Ni$ ) melts // Roik O.S., Yakovenko O.M., Kazimirov V.P., Kashyrina Y.O., Sokolskii V.E.	4
One-dimensionally confined water and ammonia molecules in single-wall carbon nanotubes // <u>Krasnov V.</u> , Druchok M., Krokhmalski T., Derzhko O.	5
Photoelastic parameters of doped potassium sulfate // Stadnyk V.Yo., Shtuka O.V., Shchepanskyi P.A.	6
Study of fluid $H_2$ under high pressure: A Generalized collective mode approach // Ilenkov I.-M., Bryk T.	7
Effect of metal deposited nanoparticles on microstructure and shear strength of lead-free solder joints // Yu. Plevachuk, V. Poverzhuk, P. Švec Sr, P. Švec, D. Janickovic, L. Orovcik, O. Bajana	8
Structural features of thermal expansion of metallic melts // Liudkevych U.I.	9
Surface tension of equiatomic InBiGaSn and InBiGaSnCu metallic melts // Ovsjanyk R. Ye., Mudry S. I., Bilyk R. M.	10
Thermodynamic quantities of Morse fluids in the supercritical region // I. V. Pylyuk, M.P. Kozlovskii, O.A. Dobush, M.V. Dufanets	12
Pseudo Jahn-Teller cooperative ordering in layered $KEr(MoO_4)_2$ induced by a magnetic fields up to 30 T // N. M. Nesterenko, K. Kutko, B. Bernáth, D. Kamenskyi	13
Bending-induced states in thin layers of van der Waals ferrielectrics // Anna N. Morozovska, Eugene A. Eliseev, Andrii V. Bodnaruk, Nicholas V. Morozovsky, Andrei L Kholkin, Yulian M. Vysochanskii, Sergei V. Kalinin	15
Polar and electrophysical properties of the nanostructure “graphene on a Janus compound ultrathin film” // Anna N. Morozovska, Andrii V. Bodnaruk, and Eugene A. Eliseev	16
Critical behavior of systems with long-range interactions and structural disorder // Maxym Dudka, Dmytro Shapoval, and Yuriy Holovatch	17
Phenomenological generalizations of conventional quantum statistical distributions // A. Rovenchak, B. Sobko	19
Phase behavior of ionic liquids in ultranarrow inhomogeneous slit pore // Maxym Dudka	20
Плазмони в металевих стрижнеподібних наночастинках із періодично модульованою бічною поверхнею // Коротун А.В.	21
Dicke model as a disordered system // Lyagushyn S.F., Sokolovsky A.I.	22
Modeling of the electrical response of random heterogeneous systems: A hard core – inhomogeneous penetrable shell model // Sushko M.Ya.	23
Thermal Conductivity Analysis for Disordered Crystals: contemporary	24



view // Horbatenko Yu. V., Krivchikov A. I., Romantsova O. O., Koroluyk O. A.	
Entanglement Entropy of Free Disordered Fermions // Pastur L.A.	26
Phase behavior of a binary mixture with Curie-Weiss interaction // M. P. Kozlovskii, O.A.Dobush	27
Nanocrystallization of amorphous alloys under the action of irradiation with argon ions // Tsaregradskaya T.L., Ovsiienko I.V., Kozachenko V.V, Kuryliuk A.M., Saenko G.V., Turkov O.V.	29
Ga-Ge-Te alloys: structural properties // Popovych M.V., Stronski A.V., Shportko K.V.	30
Effect of lattice disorder on charge transfer in PbMoO <sub>4</sub> single crystals // Bochkova T.M., Krivchenko A.Yu., Trubitsyn M.P., Volnianskii M.D., Volnyanskii D.M.	31
Crystallization of FeBSi metallic glasses annealed in an isothermal and non-isothermal way and characterized by electrical resistivity and absolute thermoelectric power // K. Khalouk, Y. Plevachuk, I. Kaban, M. Mouas, F. Gasser and J.-G. Gasser	32
Peculiarities of tape amorphous alloys surface properties // Hertsyk O.M.1, Hula T.H., Kovbuz M.O., Yezerska O.A., Kulyk Yu.O., Pandiak N.L	33
The dependence of electrical and thermoelectric properties of solid solutions AgSbSe <sub>2</sub> -PbSe on their composition // Novosad O.V. <sup>1</sup> , Shygorin P.P. <sup>1</sup> , Venhryn B.Ya. <sup>2</sup> , Shygorin O.P. <sup>1</sup>	34
Structure and mechanical properties of rapidly solidified Zr-Ni-Cr-(Al)-Ag alloys // Shved O.V.	35
Modification of the structure of amorphous metal alloys using laser processing methods // Nykyruy Yu.S., Mudry S.I., Prunitsa V.V.	36
Atomic structure and kinetics of phase formation in an amorphous metal alloy Ni <sub>83.7</sub> Fe <sub>3</sub> Cr <sub>7</sub> Si <sub>4.5</sub> B <sub>2.8</sub> during heating. // Kulyk Ju.O., Korolyshyn A.V., Velihovskij A.V.	37
Phase formation in the amorphous Fe <sub>80</sub> B <sub>20</sub> alloy during heating with alternating electric current. // S. Mudry, Yu. Kulyk, V. Prunitsa	38
Influence of the state of the C atoms on the crystal structure of martensite of carbon steels // V.A. Lobodyuk	40
Dielectric properties changing at the impurity additions and ageing in selenium-based glasses // Horvat A.A., Molnar O.O., Minkovich V.V., Mikla V.I.	41
Structural transformations and conductivity of Ni films. // Plyatsko S.V., Gromovyi Yu.S., Dmytruk N.V., Rashkovetskyi L.V., Svezhentsova K.	42
Clusterization in solutions as a process of mesophase formation // Bulavin L.A., Zabashta Yu.F., Lazarenko M.M., Vergun L.Yu., Alekseev A.N., Kovalchuk V.I., Brytan A.V.	43
Energy band gap and optical properties of CdTe spherical quantum dots calculated by DFT // Deva L.R., Semkiv I.V., Kashuba A.I., Petrus R.Y.	44
Structural transformations and optical properties of silicon oxide films	45

doped with tin // Voitovych V.V, Rudenko R.M, Poroshin V.M, Kras'ko M.M, Kolosiuk A.G, Povarchuk V.Y, Voitovych M.V	
Nanostructuring of the monocrystalline silicon surface under the action of laser pulses // Mohylyak I.A.	46
Laser-induced transformations in thermally evaporated thin TlInSe <sub>2</sub> films studied by Raman spectroscopy // Azhniuk Y. M., Gomonnai A. V., Lopushansky V. V., Gomonnai O. O., Babuka T., Loya V. Y., Voynarovych I. M.	47
Structure and Electrical Properties of $\beta$ -Ga <sub>2</sub> O <sub>3</sub> Films Obtained by Radio Frequency Magnetron Sputtering on template Si/porousSi/Si // V.V.Kidalov, A.F.Dyadenchuk, M.P.Derhachov	48
Magnetocapacitance Effect in Tunnel Contact with Perpendicular Anisotropy of Magnetic Electrodes // Konoplyuk S.M., Krupa M.M.	50
Some features of preparation 2D functional materials // Bohdan Tsizh, Stepan Mudry	51
Synthesis of ZnO photocatalyst // Klimenkov O.M., Ivanenko I.M.	52
The effect of 1 MeV electron irradiation on the array of graphene quantum dots in reduced graphene oxide in a wide temperature range of 4.2–300 K // Rudenko R.M., Voitsihovska O.O., Abakumov A.A., Bychko I.B., Poroshin V.N.	53
Collective Leggett mode in disordered two-phase superconducting ceramics // Shamaev V.V., Boliashova O.O., Tarenkov V.Yu., Shapovalov A.P.	54
Synthesis and band gap of ZnO/TiO <sub>2</sub> nanocomposites // Hutsul Kh.R., Ivanenko I.M.	55
Phase transition at critical bending of a magneto-active elastomer beam // Kalita V. M., Dzhzherya Yu. I., Cherepov S. V., Skirta Yu. B., Bodnaruk A. V., Ryabchenko S. M.	57
Electric field impact on the electrocaloric and dielectric response of the ferroelectric BaTiO <sub>3</sub> – WS <sub>2</sub> – Ag nanocomposites // Anna N. Morozovska, Oleksandr S. Pylypchuk, Andrii V. Bodnaruk, Hanna V. Shevliakova, Serhii Ivanchenko, Lesya P. Yurchenko, Eugene A. Eliseev, Nicholas V. Morozovsky and Victor V. Vainberg	58
Heat capacity and thermal expansion: analyzing of atomic, molecular crystals and carbon nanostructure systems. // M. S. Barabashko, R. M. Basnukaeva, A. I. Krivchikov, O. A. Korolyuk, A. Jeżowski	59
Features of NiC formation at mechanical alloying of the equimolar Ni-CNT and Ni-Graphite mixtures // Belyavina N.M., Ostapenko R.V., Kuryliuk A.M., Nakonechna O.I.	60
Вплив розміру і властивостей шару діелектрика на поверхневий плазмонний резонанс в 1D-структурах // Карандась Я.В., Коротун А.В., Рева В.І.	61
Плазмонні заборонені зони в нанокompозиті з хаотично розташованими металевими сфероїдальними включеннями //	62

Павлище Н.І., Коротун А.В., Тітов І.М.	
Швидкість загасання поверхневих плазмонних резонансів у сферичних металевих оболонках змінної товщини // Малиш Р.О., Коротун А.В., Рева В.І., Тітов І.М. <sup>3</sup>	63
Ionic conductivity in single-crystalline and amorphous lithium germano-germanates // A.O. Diachenko, M.P. Trubitsyn, M.D. Volnianskii, M.M. Koptiev, Ye.V. Skrypnik	64
Multi-walled carbon nanotube network on porous silicon for humidity sensing // Olenych I.B., Pavlyk M.R., Serkiz R.Ya.	65
Badanie struktur wtórnych na powierzchni tarcia powłok eutektycznych układu Fe-Mn-C-B-Si-Ni-Cr // Pashechko M.	66
Edge Luminescence of CsPbCl <sub>3</sub> Doped Single Crystals // O. Pidhornyi, Ya. Chornodolskyu, A. Pushak, O. Antonyak, T. Demkiv, R. Gamernyk, A. Voloshinovskii	67
Hybrid solder joints: Study of the thermophysical properties of solder flux with minor additions of Fe nanoparticles // Yakymovych A., Khatibi G., Wodak I., Goh Y.X.	68
Magnetoresistance and Hall effect caused by Berry curvature in Sr <sub>2</sub> FeMoO <sub>6</sub> double perovskite // Konoplyuk S.M., Krupa M.M.	69
Magnetic properties of thin films of the Gd-Fe system. // Prisyazhnyuk V.I.	70
Ab initio molecular dynamics simulation of Co-Sn melts // Kashyrina Ya.O., Muratov A.S., Roik O.S.	72
Calculation of the speed of sound in liquid Fe at high pressures via molecular dynamics simulations // Demchuk T., Bryk T.	74
Electronic properties of Mn <sup>2+</sup> doped β-LiNH <sub>4</sub> SO <sub>4</sub> crystals // Brezvin R.S., Shapravskiy A.O., Stadnyk V.Yo., Shchepanskyi P.A.	75
Computer simulations – an efficient tool for deeper understanding of experimental data of metallic melts structure. // Shtablavyi I.I., Mudry S.I.	76
Molecular dynamics simulations of the surface structure of materials in liquid and solid-liquid state. // Shtablavyi I., Plechystyy V., Popiliovskiy N., Kulyk Yu., Sembratovych N., Mudry S.	77
The trimers and dimers states in population-imbalanced fermion system // O. Hryhorchak, G. Panochko and V. Pastukhov	78